



PROCUREMENT EXECUTIVE, MINISTRY OF DEFENCE

Aeronautical Research Council  
Reports and Memoranda

STRENGTH AND ELASTIC RESPONSE  
OF SYMMETRIC ANGLE-PLY  
CARBON FIBRE REINFORCED PLASTICS

by

M.B. Snell

1978  
ROYAL AIRCRAFT ESTABLISHMENT  
BEDFORD.

London: Her Majesty's Stationery Office  
1978

PRICE £5 NET

STRENGTH AND ELASTIC RESPONSE OF SYMMETRIC ANGLE-PLY CARBON FIBRE  
REINFORCED PLASTICS

by M.B. Snell

Structures Department, RAE Farnborough

---

Reports and Memoranda No.3816\*

July 1976

---

SUMMARY

Comparisons between experimentally determined strengths and the theoretical predictions using four simple failure criteria are presented for symmetric angle-ply carbon fibre reinforced plastics laminates under tensile and compressive loads. The effects of non-linearity and failing strain are considered, and a correlation is given between the non-linear behaviour of unidirectional material subjected to shear and the non-linear elastic response of balanced angle-ply test specimens under tension.

---

\* Replaces RAE Technical Report 76091 - ARC 37230

CONTENTS

	<u>Page</u>
1 INTRODUCTION	3
2 FAILURE THEORIES	4
2.1 Quadratic interaction formulae	4
2.1.1 The Hill/Tsai criterion	4
2.1.2 The Hoffman criterion	5
2.2 Stress and strain limit theories	5
2.2.1 Theory of maximum strain	5
2.2.2 Theory of maximum stress	7
2.3 Comparison of failure theories	7
3 APPLICATION OF FAILURE THEORIES TO CFRP	8
3.1 Method of application	8
3.2 Theoretical strength curves	10
4 EXPERIMENTAL COMPARISON	11
4.1 Material fabrication	11
4.2 Specimen design	11
4.2.1 Tensile specimens	11
4.2.2 Compressive specimens	12
4.3 Testing and results	13
4.3.1 Instrumentation and test facilities	13
4.3.2 Test procedure and results	13
5 DISCUSSION	13
5.1 Comparison of experimental and theoretical strength results	13
5.2 Tensile strength results, 'scissor action' and edge effect	14
5.3 Laminate stiffness, non-linearity and failure strain	15
5.4 Correlation of angle-ply tensile and unidirectional in-plane shear responses	16
5.5 Other associated results	19
6 CONCLUDING REMARKS	19
Acknowledgments	20
Appendix Derivation of angle-ply elasticity equation	21
Table 1 Experimental compression strength data	26
Table 2 Experimental tension strength data	26
Symbols	27
References	28
Computer program - Strength	Sheets 1-10
- Angle-ply theory coefficients	Sheet 11
Illustrations	Figures 1-13
Detachable abstract cards	-

## 1 INTRODUCTION

The weight-savings obtainable from the use of carbon fibre reinforced plastics (CFRP) combined with a longer-term potential for reducing manufacturing and in-service costs have prompted UK and USA aircraft manufacturers to consider its use in significant quantities both in current aircraft and in future projects. In the General Dynamics YF16, for example, extensive use in the empennage of CFRP laminated skins yields weight savings over traditional materials of 30%.

The stiffness of multi-directional CFRP laminates is adequately determined using lamination theory<sup>1</sup> and it is relatively straightforward to design a laminate having the best required combination of Young's moduli, shear modulus and Poisson's ratios. In contrast, strength estimation for multi-directional CFRP laminates has hitherto been largely uncertain, although the recent use of various failure criteria has yielded reasonable agreement with experimental data for the strength of other composites, particularly glass/epoxy<sup>2</sup>. The shapes of the stress/strain curves and consequent strains to failure are also largely unknown for CFRP angle-ply laminates.

Several theories which predict failure of orthotropic material have been recently proposed<sup>3-8</sup>; some<sup>3-5</sup> are generalisations of the Von Mises distortional energy criterion, extended to allow for both orthotropy and different strengths in tension and compression, while others<sup>6,7</sup> are simple statements that the material will fail when the limiting stress or strain in any of the natural co-ordinate directions is reached. This Report considers four of the more relevant failure criteria and their application to CFRP laminates in angle-ply form. A comparison is made between the four theories and experimental strength data from tensile and compressive tests on CFRP balanced angle-ply laminates. Also reported is a correlation between elastic non-linearity of angle-ply test coupons in tension and the non-linearity which exists in the elastic response of unidirectional material under shear stress, and angle-ply elasticity equations are derived which relate the two. The variation of strain-to-failure with orientation for angle-ply laminates is given and a discussion deals with possible reasons for differences between the theoretically predicted values and the observed strengths of angle-ply laminates in which the ply orientations relative to the direction of the applied load are small.

## 2 FAILURE THEORIES

### 2.1 Quadratic interaction formulae

#### 2.1.1 The Hill/Tsai criterion

An isotropic medium reinforced with straight unidirectionally-aligned fibres can be considered to possess isotropy of stiffness and strength about an axis parallel with the fibres. Azzi and Tsai<sup>4</sup> used this fact in deriving a reduced form of Hill's 'plastic potential'<sup>8</sup>, proposed in 1948 to predict the yield stress in anisotropic metals. The reduced form, known as the Hill/Tsai criterion, is expressed as

$$(\sigma_1^2 - \sigma_1\sigma_2)/F_1^2 + \sigma_2^2/F_2^2 + \sigma_3^2/F_3^2 = 1 \quad (1)$$

where subscript 1 refers to directions parallel to the fibres,

subscript 2 refers to directions normal to the fibres, but in the plane of the laminate,

subscript 3 refers to shear in directions parallel to the fibres,  $F_{1,2}$  are the breaking strengths, and are either tensile or compressive according to the stress quadrant

and  $F_3$  is the breaking strength in shear.

Equation (1) represents an ellipsoidal fracture surface in  $\sigma_1, \sigma_2, \sigma_3$  space, composed of four quarter ellipsoids disposed about the  $\sigma_3$  axis. Sections parallel to the  $\sigma_1, \sigma_2$  plane appear as four quarter ellipses coincident at their points of intersection with the  $\sigma_1$  and  $\sigma_2$  axes but with discontinuous slope at these points. Representation in two axes is obtained by considering the  $(\sigma_3/F_3)^2$  term as a parameter the sole effect of which is to scale the fracture ellipse so obtained. When the shear stress on the material,  $\sigma_3$ , equals the fracture shear stress,  $F_3$ , the ellipse is reduced to a single point at the origin, indicating failure by shear with no other stress components present. At values of  $\sigma_3 < F_3$ , the theory allows additional stresses  $\sigma_1$  and  $\sigma_2$ , up to the ordinate and abscissa of the chosen point on the scaled fracture ellipse quadrant, before failure occurs. Thus any point inside the region enclosed by the fracture ellipse represents an allowable stress state and any point on or outside the bounding line represents failure of the material. An example of this criterion, applied to a high strength (HT-S) unidirectional CFRP laminate, is given in Fig.1.

### 2.1.2 The Hoffman criterion

Another modification to Hill's failure surface was proposed by Hoffman<sup>3</sup> in 1967. To cater for the possibility of different strengths in tension and compression, Hoffman included linear terms in  $\sigma_1$  and  $\sigma_2$ . This gives a continuous fracture surface with no discontinuity in slope at the axis intersections. For plane stress and transverse isotropy as before, Hoffman's criterion is

$$A1(\sigma_1^2 - \sigma_1\sigma_2) + A2\sigma_2^2 + A3\sigma_1 + A4\sigma_2 + A5\sigma_3^2 = 1 \quad (2)$$

where  $A1 = (F_{1T}F_{1C})^{-1}$ ,

$$A2 = (F_{2T}F_{2C})^{-1},$$

$$A3 = (F_{1C} - F_{1T}) / (F_{1C}F_{1T}),$$

$$A4 = (F_{2C} - F_{2T}) / (F_{2C}F_{2T})$$

$$A5 = F_3^{-2},$$

subscripts T and C indicating tension and compression respectively. With no shear stress present (i.e.  $\sigma_3 = 0$ ), and for the same unidirectional material as before, this continuous ellipse is shown on Fig.1.

## 2.2 Stress and strain limit theories

### 2.2.1 Theory of maximum strain

In the theory of maximum strain it is simply postulated that a material will fail when certain limiting values of strain are reached independent of the stress existing in the failure plane. This strain could arise due to mechanical or thermal effects. For most CFRP composites, however, little overall thermal strain will be expected and for convenience only mechanical strains are considered here.

The strain limits are obtained from uniaxial tests in the longitudinal (fibre) and transverse directions and from shear tests. These limits can then be applied under complex loading situations when the direct and Poisson's strains summate to give the total natural co-ordinate strains. Since the criterion is a simple statement that failure will occur when any of the natural co-ordinate strains reaches its limiting value, it can be written as

$$\left. \begin{aligned} \epsilon_1 &= \epsilon_{1f} , \\ \epsilon_2 &= \epsilon_{2f} \\ \epsilon_3 &= \epsilon_{3f} , \end{aligned} \right\} \quad (3)$$

and

where subscript  $f$  indicates failure. The values of  $\epsilon_{if}$ ,  $i = 1, 2, 3$ , may be obtained from uniaxial tensile, compressive and shear tests and, if linear stress/strain behaviour is assumed, the criterion may be written as

$$\epsilon_{if} = F_i/E_i . \quad (4)$$

For a linearly elastic material equation (3) can be expressed in terms of stresses, enabling the failure envelope to be compared with the other criteria on the same graph. The familiar two-dimensional stress/strain equations are

$$\left. \begin{aligned} \epsilon_1 &= \frac{\sigma_1}{E_1} - \frac{\nu_{12}}{E_1} \sigma_2 \\ \epsilon_2 &= -\frac{\nu_{12}}{E_1} \sigma_1 + \frac{\sigma_2}{E_2} . \end{aligned} \right\} \quad (5)$$

and

Substituting equation (3) in equation (5) gives

$$\left. \begin{aligned} \epsilon_{1f} &= \frac{\sigma_1}{E_1} - \frac{\nu_{12}}{E_2} \sigma_2 \\ \epsilon_{2f} &= -\frac{\nu_{12}}{E_1} \sigma_1 + \frac{\sigma_2}{E_2} , \end{aligned} \right\} \quad (6)$$

and

and substituting equation (4) in the above result yields

$$\left. \begin{aligned} \sigma_1 &= F_1 + \nu_{12} \sigma_2 \\ \sigma_2 &= F_2 + \nu_{12} \frac{E_2}{E_1} \sigma_1 . \end{aligned} \right\} \quad (7)$$

and

Equation (7), which is independent of  $\sigma_3$ , gives two pairs of parallel lines which intersect to give a stress boundary in the  $\sigma_1, \sigma_2$  plane; this is shown in Fig.1 for unidirectional material.

### 2.2.2 Theory of maximum stress

As might be expected, it is assumed in the theory of maximum stress that failure occurs when any component of the natural co-ordinate stresses reaches its limiting value. Although for a single ply this is likely to be catastrophic, for multi-directional laminates failure in the transverse direction can occur without overall collapse. The criterion is expressed as

$$\left. \begin{aligned} \sigma_1 &= F_1, \\ \sigma_2 &= F_2, \\ \sigma_3 &= F_3. \end{aligned} \right\} \quad (8)$$

and

Using the appropriate tensile or compressive strengths for unidirectional material, equation (8) is plotted on Fig.1, giving a rectangular figure with no interaction between the stresses and which is independent of shear stress,  $\sigma_3$ .

### 2.3 Comparison of failure theories

The four theories as applied to a high strength (HT-S) unidirectional laminate have been plotted on Fig.1 for zero shear stress. For the two quadratic interaction formulae, the effect of the shear stress term,  $\sigma_3/F_3$ , is to reduce the size of the ellipse while maintaining its shape. Ultimately the failure surface becomes a point at the origin, indicating failure by shear. These criteria are therefore of the distortional energy type where all deformations causing a distortion of the material, but not those causing a shape-maintaining expansion or contraction, are considered to contribute to the total strain energy of failure.

By contrast, the two limit criteria express no interaction between the direct and shear stresses and strains. They imply that the direct and shear failure stresses can each be approached independently with no loss of strength due to the presence of the other. In addition, the maximum stress theory expresses no interaction between the direct stresses, implying that the two components of direct stress can be increased to failure independently and without either mutual increase or reduction. The maximum strain theory indicates that



direct stress interaction can either increase the failing stress when Poisson's strains tend to a mutual total strain reduction, or reduce it when they cause a mutual increase.

In Fig.1 it can be seen that, for a typical high strength (HT-S) composite, there are quite large differences in the failure envelopes predicted by the four criteria in all four quadrants. It is, of course, possible that no one theory adequately describes the strength of CFRP laminates under combined stresses. An experimental programme was therefore carried out to measure the strengths of balanced angle-ply CFRP laminates in tension and compression and to compare them with the strengths derived using the four failure criteria.

### 3 APPLICATION OF FAILURE THEORIES TO CFRP

#### 3.1 Method of application

The strength of multi-ply laminates using the four failure criteria can be determined only from a knowledge of the failure surface for a single ply under stresses acting in its natural co-ordinate directions. Hence it is necessary to find the stresses acting on each ply from a knowledge of its orientation and thickness and of the in-plane laminate loading; if bending stresses are present, a knowledge of ply positions will be required also. Lamination theory (LT) is used to find the laminate compliance matrix,  $[C]$ , from which the laminate strains due to a known set of loads can be found using the equation

$$\{e_0\} = [C]\{N\} \quad (9)$$

where  $\{e_0\}$  is the column matrix of mid-plane strain components and  $\{N\}$  is the column matrix of stress resultants.

The mid-plane strain, arising from a set of stress resultants in the same ratio as the applied loads but at a level known not to cause failure, is found using equation (9). The strain in each ply natural co-ordinate direction is then found using the transformation

$$\{\gamma_n\} = T\{\gamma\}_c \quad (10)$$

where  $\{\gamma\}$  is the column matrix of tensorial strain components, subscript  $n$  indicates natural co-ordinate direction of the ply, subscript  $c$  indicates laminate reference co-ordinates,  $[T]$  is the transformation matrix.

$$\begin{bmatrix} m^2 & n^2 & 2mn \\ n^2 & m^2 & -2mn \\ -mn & mn & m^2 - n^2 \end{bmatrix}$$

where  $m = \cos \theta$

$n = \sin \theta$  and  $\theta$  is the angle of orientation of the ply.

The natural co-ordinate ply stresses are then found using the equation

$$\{\sigma\}_n = [Q]\{\varepsilon\}_c \quad (11)$$

where  $\{\sigma\}_n$  is the column matrix of natural co-ordinate stresses and  $[Q]$  is the orthotropic Hooke's law matrix for the ply.

The amplitude at failure of the known ratio of the three stress components can now be predicted for the individual ply using the four failure criteria. Under the combined stress system in which

$$\text{and } \left. \begin{aligned} \sigma_2 &= \alpha \sigma_1 \\ \sigma_3 &= \beta \sigma_1 \end{aligned} \right\}, \quad (12)$$

the Hill/Tsai criterion (equation (1)) can be solved for  $\sigma_{1f}$ , the maximum allowable level of this stress component, to give

$$\sigma_{1f} = \left( \frac{1}{F_1^2} - \frac{\alpha}{F_1^2} + \frac{\alpha^2}{F_2^2} + \frac{\beta^2}{F_3^2} \right)^{-\frac{1}{2}}. \quad (13)$$

The other two stress components at failure,  $\sigma_{2f}$  and  $\sigma_{3f}$  are then obtained from equation (12) and the laminate failure loads are found using

$$\{N\}_f = p\{N\} \quad (14)$$

where subscript  $f$  indicates failure and  $p = \sigma_{1f}/\sigma_1$ . Hoffman's criterion, equation (2), is used in the same way. The maximum strain criterion is used by first finding the smallest of the three ratios

$$q_i = \epsilon_{if} / \epsilon_i, \quad i = 1, 2, 3, \quad (15)$$

and then obtaining the failure load from

$$\{N\}_f = q_i \{N\} \quad (16)$$

where  $q_i$  is the smallest of the three ratios in equation (15). Similarly, the maximum stress theory is used to find the smallest of the three stress ratios and hence the failure load. Subroutines for each of the four criteria were programmed in FORTRAN and were used with the lamination theory program<sup>2</sup> to predict the laminate strengths. The complete strength prediction program is given in Sheets 1-10 at the end of the main text.

For the case of balanced laminates with plies at several orientations, (i.e.  $\pm\theta_1$ ,  $\pm\theta_2$  etc.) the natural co-ordinate stress and predicted failure load must be found for a single ply at each orientation. Plies at  $+\theta$  and  $-\theta$  have the same direct stress but shear stresses of opposite sign and therefore it is necessary only to predict strength from the ply with the +ve orientation. For example, a laminate consisting of balanced groups of plies at  $\pm\theta_1$ ,  $0^\circ$ ,  $\pm\theta_2$  would be analysed by considering the failure loads of  $+\theta_1$ ,  $0^\circ$  and  $+\theta_2$  plies only. In such cases it would usually be found that the plies in a single orientation will fail before the others. Assumptions must then be made as to the effect of the failed group of plies on the strength of the laminate as a whole. In this Report only simple angle-ply laminates are considered in detail (i.e.  $\pm\theta$  only) and the laminate failure load is determined from the failure of any one ply.

### 3.2 Theoretical strength curves

The four theories were first used to predict the compressive strength of high modulus (HM-S) angle-ply laminates using strength and stiffness data for uni-directional material obtained from the  $0^\circ$ ,  $90^\circ$  and  $\pm 45^\circ$  strength results of the present series of compression tests and a previously measured value of in-plane transverse tensile strength of  $50\text{MN/m}^2$ , and curves were prepared which show the variation of compressive strength with orientation (see Fig.2). Similar curves were drawn to predict tensile strength of high strength (HT-S) angle-ply laminates (see Fig.7). As can be seen, the differences in the predicted strengths from the four theories are large, especially in the region between  $\pm 10^\circ$  and  $\pm 35^\circ$ . Furthermore, in the region between  $\pm 20^\circ$  and  $\pm 40^\circ$ , where there is considerable shear acting, the differences between the quadratic interaction

formulae and the limit theories are greatly accentuated since the latter take no account of the effect of shear stress on failure. This was effectively demonstrated by running the Hill/Tsai subroutine with the shear interaction term deleted which, between  $\pm 25^\circ$  and  $\pm 35^\circ$ , gave results close to those of the maximum strain theory.

In addition to the predictions of failure load, the two limit theories indicate the modes of failure. On Fig.3, which shows the variation of compressive strength with orientation according to the maximum strain theory, four distinct modes of failure can be identified. Mode 1 is compressive failure in the fibre directions which, perhaps surprisingly, is replaced at orientations of around  $15^\circ$  by a second mode indicating failure due to transverse tension; this is principally a result of the very high Poisson's ratio ( $>1.5$ ) which exists between  $\pm 15^\circ$  and  $\pm 35^\circ$  for this particular material. Mode 3, between  $\pm 35^\circ$  and  $\pm 75^\circ$ , indicates shear failure and is succeeded by a fourth mode, transverse compression. In practice it is possible to identify only three separate modes from examination of the failure surfaces, since modes 2 and 3 are difficult to differentiate.

The two interaction formulae can give only the distinction between a shear and a non-shear failure and give continuous curves rather than mode segments.

#### 4 EXPERIMENTAL COMPARISON

##### 4.1 Material fabrication

The laminated boards were made from pre-impregnated sheets, nominally 0.25mm cured thickness at 0.6 fibre volume fraction, supplied by Rotorway Components Ltd. The resin system used was ERLA4617/DDM. Both high modulus (HM-S) and high strength (HT-S) laminates were fabricated using a method similar to that used by Collings and Ewins<sup>9</sup> and were cured between the heated plattens of an hydraulic press to a thickness close to that required for a fibre volume fraction of 0.6. The high modulus (HM-S) laminates were of 2mm nominal thickness and were made at  $15^\circ$  intervals from  $0^\circ$  to  $90^\circ$  with the balanced stacking sequence  $+0, -0, +0, -0, -0, +0, -0, +0$ . The high strength (HT-S) laminates were made at  $5^\circ$  intervals from  $0^\circ$  to  $50^\circ$  and also at  $90^\circ$ , and were of 1mm thickness and laid in the sequence  $+0, -0, -0, +0$ .

##### 4.2 Specimen design

###### 4.2.1 Tensile specimens

In tensile testing, the main requirements are a uniform stress field in the specimen gauge length, elimination of bending strains and the minimisation of the

three-dimensional edge effects<sup>10</sup> which occur in angle-ply specimens. Specimens were therefore chosen to be long enough to ensure a uniform stress field according to St. Venant's principle; this also reduced the effect of any bending strains induced by the testing apparatus. Sufficient width is required in order that edge effects, extending inwards for approximately one specimen thickness, become an insignificant proportion of the stress field in the failure region. A minimum width of 20mm was considered adequate for the thickness of 1mm. To allow full freedom of action for modes of failure involving shear displacements, some of the specimens had freely pinned ends and were loaded by steel links. This also eliminated any possible bending in the width.

Failure was limited to the specimen centre by symmetrically grinding a waisted profile using a 200mm diameter grinding wheel. The basic strip width of 30mm was reduced to 20mm over a gauge length of 20mm. The tensile specimen geometry is illustrated in Fig.4.

#### 4.2.2 Compressive specimens

In addition to the requirements for the tensile testing of coupon specimens given in section 4.2.1, compressive strength testing introduces the problem of instability which must be eliminated by the choice of a suitable specimen. For maximum resistance to overall buckling, encastré type end fittings were used, which effectively prevented any end rotation. The criterion used for buckling was the Euler equation factored by 0.9 (a 10% reduction) to allow adequately for transverse shear flexibility. The factored Euler equation is

$$P_c = \frac{3.6\pi^2 E_x I}{l^2} \quad (17)$$

where  $I = \frac{\omega t^3}{12}$  ,

$\omega$  is the coupon width,

$t$  is the coupon thickness

and  $l$  is the length between the end fittings.

The variation in modulus ( $E_x$ ) with orientation made it necessary to reduce the length from 30mm at 0° to 5mm at ±90° orientation according to equation (17). the failure position was controlled by symmetrically grinding a circular arc profile which reduced the width by 5mm to 15mm. For each specimen length the arc radius was chosen so that the profile occupied a distance slightly greater than the built-in length. The compressive specimens are illustrated on Fig.4.

### 4.3 Testing and results

#### 4.3.1 Instrumentation and test facilities

The complete load/strain history for the tensile specimens was plotted during the tests using an X-Y recorder. The strain-proportional input to the recorder was derived from the out-of-balance signal from a singly-active Wheatstone bridge circuit with a foil strain gauge as the active element. The load-proportional input was obtained from an integral potentiometer, the wiper arm of which was connected to the load indicating needle of the mechanical test machine. Bridge excitation was 6V with a very low ripple component of <0.5mV peak-to-peak to eliminate oscillation of the X-axis pen. Input to the test machine potentiometer was 1.5V. The mechanical tests were carried out on an Avery Universal Testing Machine of 100kN capacity.

#### 4.3.2 Test procedure and results

The specimens were tested by steadily increasing the load up to failure over a period of about one minute. The load/strain curves recorded from the tensile tests were mostly smooth, although for some specimens small step-like irregularities in the curve were recorded due to the slower rate of response of the load sensor compared with that of the strain gauge. The modes of failure of all specimens were identified from visual examination of the failed surfaces. The test results are given in Tables 1 and 2, and representative stress/strain curves are given in Figs.5 and 6.

## 5 DISCUSSION

### 5.1 Comparison of experimental and theoretical strength results

Fig.3 gives the variation of compressive strength with orientation for balanced, high modulus (HM-S) angle-ply laminates at a nominal fibre volume fraction of 0.6. Agreement between experiment and theory is best for the maximum strain theory, with the interaction formulae underestimating the strength at orientations up to  $\pm 40^\circ$ . Exact agreement between experiment and all theories at  $0^\circ$  and  $90^\circ$  is obtained since the experimental results at these orientations are used as input data to predict the strength at all other orientations. At  $\pm 45^\circ$ , where strength is equal to twice the in-plane shear strength, agreement is also exact; the reasons for such agreement are dealt with more fully in section 5.3.

The theoretical prediction of the four failure criteria for the tensile strength of high strength (HT-S) laminates is given in Fig.7 and the comparison between the maximum strain theory and experiment is given in Fig.8. Close

agreement cannot be demonstrated, except in the region of shear failures at around  $\pm 45^\circ$  and of course at the end points ( $0^\circ$  and  $90^\circ$ ). However, some reasons why good agreement with the failure criteria was obtained from the compressive strength tests but not from the tensile strength tests can be suggested, which result from the practically available tensile specimens being of inadequate design (see section 5.2). Low strength values were obtained from the tensile specimens at small values of  $\theta$  because, at the high stress levels existing at failure, load was not transmitted adequately into the fibres. This was shown by the failure mode of these specimens which exhibited in-plane and interlaminar cracking without fibre failure. Load transfer from the test-machine wedge-grips into the specimen gauge length is by shear in the resin matrix and at the matrix/fibre interface. This mechanism, compounded with edge effect, is inadequate to transmit the high loads required to fail the high strength (HT-S) fibres of the tensile specimens. By contrast the compressive specimens, being of high modulus (HM-S) fibres in which the fibres fail at about half the stress of the high strength (HT-S) fibres, require only half as much internal stress to achieve the fibre breaking load. Further, the load path for the low-orientation compressive specimens is principally through direct pressure on the fibre ends with a much reduced shear transfer requirement. The types of failure observed for these specimens indicate that the load transfer mechanism was adequate to achieve fibre failure. Agreement with a failure criteria based on single ply strength values was therefore possible and it was found that good agreement was obtained with the strengths and modes given by the maximum strain criterion.

## 5.2 Tensile strength results, 'scissor action' and edge effect

The measured tensile strength results are shown on Fig.8, together with the theoretical prediction of the maximum strain theory, which was again found to give best agreement. No theory gave good agreement at small angles of orientation between  $\pm 5^\circ$  and  $\pm 15^\circ$ , indeed at  $\pm 10^\circ$  only about half of the predicted value was achieved. Between  $\pm 20^\circ$  and  $\pm 50^\circ$ , in a region largely of shear mode failures, agreement between the predicted modes and strengths and the measured results is good while at  $90^\circ$  agreement is of course exact, this being a value used in the prediction of the strength curve.

Two reasons for the low strength results between  $\pm 5^\circ$  and  $\pm 15^\circ$  can however be suggested, which, although they apply to both tensile and compressive specimens, are likely to be more significant for high strength (HT-S) laminates because of the higher internal stresses. When fibres are symmetrically angled

about the loading axis, the material becomes trellis-like in its structure and, under tensile load, rotations about the almost infinite number of intersections of fibres tend to cause a 'scissor action' type of twisting between the plies, so reducing the orientation angle. This is manifest in the very high Poisson's ratios of up to 2.0 which are predicted by lamination theory and are measured in practice. High transverse stresses and strains are inevitably induced which contribute to failure at relatively low laminate strain. Another cause of early failure may be the interlaminar stresses,  $\tau_{xz}$ ,  $\tau_{yz}$  and  $\sigma_z$  (see Fig.9), which occur in the edge regions. The interlaminar shear stress in the edge region is reported<sup>10</sup> to rise rapidly with orientation and to have reached at least 75% of its maximum value (which occurs at  $\pm 35^\circ$ ) in the region between  $\pm 15^\circ$  and  $\pm 50^\circ$ . Most of the failures at low orientation (i.e.  $< \pm 20^\circ$ ) were of an indeterminate mode, but since considerable interlaminar separation and cracking were present it is probable that interlaminar stresses have adversely affected the measured strength. The edge effect would of course disappear in a specimen without free edges and the experimental tensile strength results between  $\pm 5^\circ$  and  $\pm 15^\circ$  serve only as a lower bound to the true tensile strength of the material. Nevertheless the results are a useful indicator of the large reductions in strength which can result from the influence of a free edge. It was noticed that the failure stress of specimens twice the width of those described was slightly higher, indicating that edge effects were indeed affecting the results. The upper width limit, beyond which there is no further strength increase, is difficult to find in practice because of both the scale of specimen required to furnish sufficient aspect ratio for uniform stress and the sensitivity of such specimens to widthwise bending. In any case, the upper strength limit will still be influenced by edge effects and probably the only way to find the true strength is to use a specimen without free edges, such as a tube.

### 5.3 Laminate stiffness, non-linearity and failure strain

The strain gauging of the tensile specimens enabled a check to be made of the theoretical modulus using lamination theory for the various ply orientations and also gave the full stress/strain curves up to failure. The comparison between the theoretical and experimental moduli at low strain is given in Fig.10 and the very good agreement is further evidence of the accuracy of the theory for small strains. Representative stress/strain curves given in Figs.5 and 6 show that from  $\pm 30^\circ$  to  $\pm 45^\circ$  non-linearity is marked and increasing. At high strain levels linear analyses are therefore inadequate to deal with laminates composed solely of plies at such orientations and deformations are always underestimated



for stresses above the linear region. The variation of the measured failure strain with orientation is given in Fig.11, together with a possible theoretical comparison based on linear elasticity. As can be clearly seen, the non-linear effects greatly increase strains at failure and limit the application of the theory to the initial linear response. It was noticed that, for the four instances in which the load was released before failure took place, the non-linear curves were almost completely elastically recoverable with very little permanent strain. This indicates that the material is non-linearly elastic for the low strain rates considered and not visco-elastic as might be implied from the relatively high degree of non-linearity. It is possible that the non-linear effects are due to the non-linearity in shear and this is considered in detail in the following section.

#### 5.4 Correlation of angle-ply tensile and unidirectional in-plane shear response

Earlier work<sup>11</sup> on unidirectional in-plane shear properties had indicated considerable shear stress non-linearity and, because of the high shear stress acting on planes parallel to the fibre directions of  $\pm 45^\circ$  angle-ply tensile specimens, it was thought that the tensile and shear non-linearities might be directly connected. A theoretical analysis was carried out which enabled the complete tensile stress/strain curve to be plotted using unvarying values of  $E_1$ ,  $E_2$  and  $\nu_{12}$  together with ordinates and abscissae from the experimentally derived non-linear shear stress/strain curve. A computer program, given in Appendix C, was written to calculate the results. Results identical to lamination theory for the linear portion were obtained, providing a check on the angle-ply analysis. A summary of the more important results derived from the analysis follows, although the detailed derivations are given in the Appendix.

For balanced angle-ply laminates the natural co-ordinate stresses can be expressed in terms of natural co-ordinate shear stress and strain by equations of the form

$$\text{and } \left. \begin{aligned} \sigma_1 &= A_1 \tau_{12} + A_2 \gamma_{12} \\ \sigma_2 &= B_1 \tau_{12} + B_2 \gamma_{12} \end{aligned} \right\} \quad (18)$$

where the coefficients  $A_1$ ,  $A_2$  etc. are functions both of the orthotropic parameters  $E_1$ ,  $E_2$  and  $\nu_{12}$  and of fourth order multiples of  $\sin \theta$  and  $\cos \theta$  (see the Appendix). On transforming equations (18) the laminate applied load becomes

$$\sigma_x = A_7 \tau_{12} + A_8 \gamma_{12} . \quad (19)$$

The natural co-ordinate strains can be expressed as

$$\text{and } \left. \begin{aligned} \epsilon_1 &= A_3 \tau_{12} + A_4 \gamma_{12} \\ \epsilon_2 &= B_3 \tau_{12} + B_4 \gamma_{12} , \end{aligned} \right\} \quad (20)$$

and the laminate strain as

$$\epsilon_x = A_5 \tau_{12} + A_6 \gamma_{12} . \quad (21)$$

Thus equations (19) and (21) can be used to predict the tensile stress/strain curve using the coefficients  $A_1, A_2, B_1, B_3$  etc., assumed constant and a measured shear stress/strain curve for unidirectional material.

At  $\theta = 45^\circ$ , the stresses cease to be functions of shear strain so that

$$\sigma_1 = \frac{2(\nu_{12} E_2 + E_1) \tau_{12}}{E_1 + E_2 + 2\nu_{12} E_2} \quad (22)$$

and

$$\sigma_2 = \frac{2E_2(1 + \nu_{12}) \tau_{12}}{E_1 + E_2 + 2\nu_{12} E_2} , \quad (23)$$

which together yield

$$\sigma_x = 2\tau_{12} \quad (24)$$

and

$$\epsilon_x = \frac{2(E_1 - \nu_{12}^2 E_2)}{E_1(E_1 + E_2 + 2\nu_{12} E_2)} \tau_{12} + \frac{\gamma_{12}}{2} . \quad (25)$$

It is of considerable interest that the above equations can also be used to determine the initial value of  $G_{12}$  from the tensile test results. In the linear portion of the shear stress/strain curve,  $\tau_{12}$  and  $\gamma_{12}$  are related by

$$G_{12} = \tau_{12} / \gamma_{12} . \quad (26)$$

Strain transformation at  $\theta = 45^\circ$  results in

$$\gamma_{12} = -\epsilon_x + \epsilon_y \quad (27)$$

and since

$$\epsilon_y = -\nu_{xy}\epsilon_x \quad (28)$$

then

$$\gamma_{12} = \epsilon_x(1 + \nu_{xy}) \quad (29)$$

Substituting equations (24) and (29) in equation (26) yields,

$$G_{12} = \frac{\sigma_x}{\epsilon_x 2(1 + \nu_{xy})} \quad (30)$$

or

$$G_{12} = \frac{E_x}{2(1 + \nu_{xy})} \quad (31)$$

It should be noted that this remarkable result, also obtained by a different route<sup>12</sup>, although applicable throughout the whole elastic region, should only be used for the linear portion in the determination of the unvarying value of  $G_{12}$  (equation (26)). Equation (31) enables the in-plane shear modulus,  $G_{12}$ , to be simply determined from a tensile test on a  $\pm 45^\circ$  balanced specimen with two strain gauges attached for the determination of  $E_x$  and  $\nu_{xy}$ . Although rough checks of equation (31) using existing data have yielded reasonable agreement, rigorous experimental verification remains to be done.

On the assumption that the three orthotropic parameters  $E_1$ ,  $E_2$  and  $\nu_{12}$  do not vary with load (an assumption verified in practice), it is also possible to predict the tensile stress/strain curve for angle-ply laminates using the measured shear stress/strain curve for unidirectional material. This was done at  $\theta = 35^\circ$  using equations (19) and (21) and at  $\theta = 45^\circ$  using equations (24) and (25) and the results are given in Fig.12.

Throughout this analysis it has been assumed that the normal stress,  $\sigma_2$ , and the parallel shear stress,  $\tau_{12}$ , are independent. Although this is thought to be true as far as stiffness is concerned, evidence<sup>13,14</sup> exists which indicates that normal stress influences shear strength; compression tends to increase and tension to decrease the shear strength. The statement that in-plane shear strength,  $F_{12}$ , equals half the tensile strength,  $F_x$ , at  $\pm 45^\circ$  must therefore be qualified by the fact that normal tensile stress exists on the failure plane given by equation (23) as

$$\frac{\sigma_2}{\tau_{12}} \approx 0.1 \quad .$$

However this low percentage of normal tensile stress appears to have little effect on the shear strength<sup>13</sup> and it seems that the result,

$$F_{12} = F_x/2, \quad (32)$$

can be used to determine the in-plane shear strength of unidirectional material.

### 5.5 Other associated results

The accuracy of equation (31) in predicting the initial value of  $G_{12}$  would be impaired if  $G_{12}$  were to be highly sensitive to changes in the independent variables. The degree of sensitivity was investigated by plotting equation (31) with  $E_x$  constant, for a typical high strength (HT-S) angle-ply laminate at  $\pm 45^\circ$ . Fig.13 gives the result which shows that in the region of practical values of  $G_{12}$ , when  $\nu_{xy}$  varies between 0.7 and 0.9,  $G_{12}$  varies between 5.3 and 4.7GN/m<sup>2</sup>. Accurate measurements of  $\nu_{xy}$  must therefore be made if accurate values of  $G_{12}$  are to be derived.

Further consideration of the complete curve shows that  $\nu_{xy}$  decreases with  $G_{12}$  until, at  $G_{12} = 8.9\text{GN/m}^2$ ,  $\nu_{xy} = 0$ ; for greater values of  $G_{12}$ ,  $\nu_{xy}$  becomes negative. It is unlikely that these effects would ever be realised in practice, however, since the combination of high shear stiffness, high fibre stiffness and low transverse direct stiffness which is required would probably never be encountered.

## 6 CONCLUDING REMARKS

The variation of compressive and tensile strength with fibre orientation has been obtained both experimentally and theoretically for symmetric CFRP angle-ply laminates. It has been shown that, particularly in the case of tensile stress on high strength (HT-S) laminates, there is a large and theoretically unpredicted reduction in strength whenever the fibres are at small angles from the loading axis. The reason for using angle ply construction is to increase the shear and transverse stiffness and strength, but in so doing there is a large sacrifice in longitudinal strength. A better type of construction might be to use a proportion of fibres in the two principal loading directions to carry the direct loads, and a proportion of symmetric layers at  $\pm 45^\circ$  to carry shear loads.

It has also been shown that non-linearity and failure strain increase with orientation up to  $\pm 40^\circ$  where they are a maximum and thereafter decrease, the response becoming linear at angles greater than about  $\pm 50^\circ$ .

Shear and tensile effects have been related, and a simple method of determining the shear modulus,  $G_{12}$ , has been given. The correlation between the direct stress on symmetric angle-ply laminates with ply orientations of  $\pm 45^\circ$  and the unidirectional shear stress should prove useful in shear property characterisation.

#### Acknowledgments

Thanks are due to my colleagues, Dr. P. Bartholomew for assistance with the angle-ply equations and Mr. D. Purslow for the use of his shear data.

Appendix

DERIVATION OF ANGLE-PLY ELASTICITY EQUATIONS

A.1 Equilibrium

Referring to Fig.9, the following equilibrium equations apply

$$\sigma_x^a = \sigma_1 \cos^2 \theta + \sigma_2 \sin^2 \theta + 2\tau_{12} \sin \theta \cos \theta \quad (A-1)$$

$$\sigma_y^a = \sigma_1 \sin^2 \theta + \sigma_2 \cos^2 \theta - 2\tau_{12} \sin \theta \cos \theta \quad (A-2)$$

$$\tau_{xy}^a = -\sigma_1 \sin \theta \cos \theta + \sigma_2 \sin \theta \cos \theta + \tau_{12}(\cos^2 \theta - \sin^2 \theta) \quad (A-3)$$

where superscript a applies to the  $+\theta$  ply direction.

For the  $-\theta$  ply direction (superscript b),

$$\sigma_x^b = \sigma_1 \cos^2 \theta + \sigma_2 \sin^2 \theta + 2\tau_{12} \sin \theta \cos \theta, \quad (A-4)$$

$$\sigma_y^b = \sigma_1 \sin^2 \theta + \sigma_2 \cos^2 \theta - 2\tau_{12} \sin \theta \cos \theta \quad (A-5)$$

and

$$\tau_{xy}^b = \sigma_1 \sin \theta \cos \theta - \sigma_2 \sin \theta \cos \theta - \tau_{12}(\cos^2 \theta - \sin^2 \theta). \quad (A-6)$$

Adding equations (A-1) and (A-4) gives the relationship between the applied load and the ply internal stresses,

$$\sigma_x = \sigma_1 \cos^2 \theta + \sigma_2 \sin^2 \theta + 2\tau_{12} \sin \theta \cos \theta, \quad (A-7)$$

$$\sigma_y = \sigma_1 \sin^2 \theta + \sigma_2 \cos^2 \theta - 2\tau_{12} \sin \theta \cos \theta = 0 \quad (A-8)$$

and

$$\sigma_{xy} = 0. \quad (A-9)$$

A.2 Compatibility

Because there is an equal number of plies at  $-\theta^0$  as at  $+\theta^0$ , shear strain  $\gamma_{xy}$  is eliminated and so

$$\gamma_{xy} = 0. \quad (A-10)$$

This leads to

$$2 \sin \theta \cos \theta (-\epsilon_1 + \epsilon_2) + (\cos^2 \theta - \sin^2 \theta)\gamma_{12} = 0. \quad (A-11)$$

### A.3 Elasticity

The orthotropic elasticity equations, relating the natural co-ordinate stresses and strains, can be expressed as

$$\epsilon_1 = \frac{\sigma_1}{E_1} - \frac{\nu_{21}\sigma_2}{E_2} \quad (\text{A-12})$$

and

$$\epsilon_2 = \frac{\sigma_2}{E_2} - \frac{\nu_{12}\sigma_1}{E_1} \quad (\text{A-13})$$

### A.4 Derivation

Substitution of equations (A-12) and (A-13) in equation (A-11) results in

$$- 2/E_1(1 + \nu_{12})\sigma_1 SC + 2(\nu_{12}/E_1 + 1/E_2)\sigma_2 SC = - \gamma_{12}(C^2 - S^2) \quad (\text{A-14})$$

where S and C are abbreviations for  $\sin \theta$  and  $\cos \theta$ . This equation, together with equation (A-8), enables  $\sigma_1$  and  $\sigma_2$  to be expressed in terms of  $\tau_{12}$  and  $\gamma_{12}$ , the results for which are

$$\sigma_1 = \frac{2SC\tau_{12}}{\frac{(1 + \nu_{12})E_2}{\nu_{12}E_2 + E_1} C^2 + S^2} + \frac{C^2(C^2 - S^2)\gamma_{12}}{\frac{2(1 + \nu_{12})}{E_1} SC^3 + 2\left(\frac{\nu_{12}E_2 + E_1}{E_1E_2}\right)S^3C} \quad (\text{A-15})$$

By setting

$$\frac{E_2(1 + \nu_{12})}{\nu_{12}E_2 + E_1} = A,$$

$$\frac{\nu_{12}E_2 + E_1}{E_1E_2} = B$$

and

$$\frac{1 + \nu_{12}}{E_1} = D,$$

equation (A-15) becomes

$$\sigma_1 = \frac{2SC\tau_{12}}{AC^2 + S^2} + \frac{C^2(C^2 - S^2)\gamma_{12}}{2DSC^3 + 2BS^3C}, \quad (\text{A-16})$$

and further abbreviation yields

$$\sigma_1 = A_1\tau_{12} + A_2\gamma_{12} \quad (\text{A-17})$$

where  $A_1 = \frac{2SC}{AC^2 + S^2}$

and  $A_2 = \frac{C^2(C^2 - S^2)}{2DSC^3 + 2BS^3C}$ .

Similarly,

$$\sigma_2 = \frac{2SC\tau_{12}}{C^2 + S^2/A} - \frac{S^2(C^2 - S^2)\gamma_{12}}{2DSC^3 + 2BS^3C} \quad (\text{A-18})$$

which is abbreviated to

$$\sigma_2 = B_1\tau_{12} + B_2\gamma_{12} \quad (\text{A-19})$$

where  $B_1 = \frac{2SC}{C^2 + S^2/A}$

and  $B_2 = \frac{S^2(C^2 - S^2)}{2DSC^3 + 2BS^3C}$ .

Equations (A-17) and (A-19) are used to express the natural co-ordinate strain components  $\epsilon_1$  and  $\epsilon_2$  in terms of  $\tau_{12}$  and  $\gamma_{12}$ . Their substitution in equation (A-12) results in

$$\epsilon_1 = A_3\tau_{12} + A_4\gamma_{12} \quad (\text{A-20})$$

where  $A_3 = A_1/E_1 - \nu_{12}B_1/E_1$

and  $A_4 = (A_2 - \nu_{12}B_2)/E_1$ ,



and

$$\epsilon_2 = B_3 \tau_{12} + B_4 \gamma_{12} \quad (\text{A-21})$$

where  $B_3 = B_1/E_2 - \nu_{12}A_1/E_1$

and  $B_4 = B_2/E_2 - \nu_{12}A_2/E_1$  .

The two natural co-ordinate direct strains are used to express the laminate strain in terms of  $\tau_{12}$  and  $\gamma_{12}$  . Strain transformation yields

$$\epsilon_x = \epsilon_1 \cos^2 \theta + \epsilon_2 \sin^2 \theta + \gamma_{12} \sin \theta \cos \theta \quad (\text{A-22})$$

and

$$\epsilon_y = \epsilon_1 \sin^2 \theta + \epsilon_2 \cos^2 \theta - \gamma_{12} \sin \theta \cos \theta \quad (\text{A-23})$$

Hence equations (A-20) and (A-21) are substituted in equation (A-22) to give

$$\epsilon_x = (A_3 CC + B_3 SS) \tau_{12} + (A_4 CC + B_4 SS + SC) \gamma_{12} \quad (\text{A-24})$$

which is abbreviated to

$$\epsilon_x = A_5 \tau_{12} + A_6 \gamma_{12} \quad (\text{A-25})$$

where  $A_5 = A_3 CC + B_3 SS$

and  $A_6 = A_4 CC + B_4 SS + SC$  .

Similarly, equation (A-23) yields

$$\epsilon_y = (A_3 SS + B_3 CC) \tau_{12} + (A_4 SS + B_4 CC - SC) \gamma_{12} \quad (\text{A-26})$$

Hence

$$\epsilon_y = B_5 \tau_{12} + B_6 \gamma_{12} \quad (\text{A-27})$$

where  $B_5 = A_3 SS + B_3 CC$

and  $B_6 = A_4 SS + B_4 CC - SC$  .

Equations (A-25) and (A-27) enable Poisson's ratio for the laminate to be determined. For the straight line portion of the shear stress/strain curve where  $G_{12}$  is constant,

$$G_{12} = \tau_{12}/\gamma_{12} . \quad (A-28)$$

Equation (A-28), when substituted in equations (A-25) and (A-27), gives equations for  $\epsilon_x$  and  $\epsilon_y$  which yield the expression for Poisson's ratio,

$$\nu_{xy} = \epsilon_y/\epsilon_x = (B_5G_{12} + B_6)/(A_5G_{12} + A_6) . \quad (A-29)$$

The laminate stress is found from equation (A-4) by substitution of equations (A-17) and (A-19). This results in

$$\sigma_x = A_7\tau_{12} + A_8\tau_{12} \quad (A-30)$$

where  $A_7 = A_1CC + B_1SS + 2SC$

and  $A_8 = A_2CC + B_2SS$  .

Table 1  
ANGLE-PLY COMPRESSION STRENGTH (HM-S/ERLA 4617/DDM)

Orientation + - + - - + - + (degrees)	Fibre volume fraction ( $v_f$ )	Number of specimens	Average strength ( $\text{MN/m}^2$ )	Mode of failure
0	All specimens fell between 0.58 and 0.61	3	605	Longitudinal compression
15		3	524	Longitudinal compression
30		3	265	Transverse tension
45		3	140	Shear
60		3	175	Shear
75		3	185	Transverse compression
90		3	152	Transverse compression

Table 2  
ANGLE PLY TENSION STRENGTH (HM-S/ERLA 4617/DDM)

Orientation + - - + (degrees)	Thickness (mm)	Number of specimens	Average strength ( $\text{MN/m}^2$ )	Coeff. of variation %	Response/failure mode
0	1.1	5	1017	8.99	Linear/tensile, shear cracks
5	1.08	7	745	6.64	Linear/tensile, shear cracks
10	1.08	7	536.4	9.70	Linear/brittle, indeterminate
15	1.1	7	509	8.31	Linear/tensile
20	1.1	7	426.8	9.26	Linear/tensile
25	1.1	7	405	2.79	Non-linear/tensile
30	1.12	7	339.7	7.69	Non-linear/tensile
35	1.1	7	310	3.04	Non-linear/tensile
40	1.2	5	140	10.0	Non-linear/shear
45	1.1	7	106.4	4.98	Non-linear/shear
50	1.14	5	70.2	4.77	Non-linear/shear
90	1.1	3	28.6	8.73	Linear/tensile

SYMBOLS

E	Young's modulus
F	breaking stress
$G_{12}$	shear modulus of unidirectional material
$l$	specimen length between and fittings
p	failure stress multiplier
q	failure strain ratio
t	strength specimen thickness
$v_f$	fibre volume fraction
w	strength specimen width
$\alpha, \beta$	natural co-ordinate stress ratios
$\gamma_{12}$	in-plane, fibre parallel engineering shear strain
$\epsilon$	engineering strain
$\theta$	angular orientation from the reference direction
$\nu$	Poisson's ratio
$\sigma$	stress
$\tau_{12}$	in-plane fibre-parallel shear stress
[C]	$3 \times 3$ compliance matrix
[N]	$3 \times 1$ column of loads per unit length
[T]	$3 \times 3$ co-ordinate transformation matrix
[Q]	$3 \times 3$ matrix of orthotropic stiffness components
$[\epsilon_0]$	$3 \times 1$ column matrix of mid-plane strain components
$[\gamma]$	$3 \times 1$ column of tensional strain components

Subscripts

1	fibre-parallel direction
2	direction normal to the fibres, in the laminate plane
3	refers to fibre-parallel shear
C	compression
c	indicates that terms are in laminate reference co-ordinates
f	failure
n	indicates that terms are in natural co-ordinate (1,2,3) directions
0	refers to conditions at laminate mid-plane
T	tension
x,y,z	laminate reference co-ordinate directions

REFERENCES

<u>No.</u>	<u>Author</u>	<u>Title, etc</u>
1	M.B. Snell	The stiffness of orthotropic laminated plates. RAE Technical Report 75002 (ARC 36085) (1975)
2	S.W. Tsai	Strength characteristics of composite materials. NASA CR-224 (1965)
3	O. Hoffman	The brittle strength of orthotropic materials. J. Composite Materials, Vol.1, pp.200-206 (1967)
4	V.D. Azzi S.W. Tsai	Anisotropic strength of composites. Experimental Mechanics, pp.283-288, September 1965
5	J. Marin	Theories of strength for combined stresses and non-isotropic materials. Journal of Aeronautical Sciences, Vol.24, pp.265-268, April 1957
6	C.F. Jenkin	Report on materials of construction used in aircraft and aircraft engines. London Aeronautical Research Committee (1920)
7	A.S.T.M.	Composite materials: testing and design, p.164. Philadelphia ASTM Special Technical Publication 460 (1969)
8	R.W. Hill	A theory of yielding and plastic flow of anisotropic metals. Proc. Roy. Soc., Series A, Vol.193, pp.281-297 (1948)
9	T.A. Collins P.D. Ewins	Tensile and compressive strength measurements on some unidirectional carbon fibre reinforced plastics. RAE Technical Report 72063 (1972)
10	R.B. Pipes N.J. Pagano	Interlaminar stresses in composite laminates under axial extension. J. Comp. Materials, Vol.4, pp.538-548 (1970)
11	D. Purslow	The shear properties of unidirectional carbon fibre reinforced plastics and their experimental determination. ARC CP No.1381 (July 1976)
12	H.T. Hahn	A note on the determination of the shear stress-strain responses of unidirectional composites. J. Composite Materials, Vol.7, pp.383-386 (July 1973)

REFERENCES (concluded)

<u>No.</u>	<u>Author</u>	<u>Title, etc</u>
13	N.J. Wadsworth J. Hutchings	Transverse properties of carbon fibre/resin composites. RAE Technical Report 67099 (1967)
14	T.A. Collings	The transverse compressive behaviour of unidirectional carbon fibre reinforced plastics. RAE Technical Report 72237 (ARC 34592) (1972)

## Program listing

## Strength

```

MASTER STRENGTH
  DIMENSION E11(100),E22(100),ANU12(100),ANU21(100),G12(100),TH(100)
1, THFTAD(100), THETAR(100), Q11(100), Q12(100), Q22(100), Q66(100),
2H(100), Q11B(100), Q12B(100), Q16B(100), Q22B(100), Q26B(100), A(3,3),
3B(3,3), C(6,6), RO(100), D(3,3), AMA(100), AA(3,3), CC(6,6), R1(100),
4R2(100), R3(100), R4(100), R5(100), R6(100), RM(3,3), AB(3,3), BA(3,3),
5BB(3,3), DB(3,3), Q66B(100)
  DIMENSION S(3), ES(3), U(100), T(3,3), EN(3), Q(3,3), SN(3)
  DIMENSION X(1000), Y(1000), LX(1000), LY(1000), TP(120), TX(1000),
1TY(1000)
  COMMON/R1/FT1,FC1,FT2,FC2,F12/B2/AE,HE,BE,GE,FE,CE,HAE,HHE,HBE/
1B3/PI/B4/SN,S/B5/X,Y,NXY/B6/D5/B7/EN/B8/EE1,EE2,EE3
  READ(1,90) FT1,FC1,FT2,FC2,F12
  WRITE(2,102) FT1,FC1,FT2,FC2,F12
  READ(1,90) S(1),S(2),S(3)
  WRITE(2,102) S(1),S(2),S(3)
  PI = 8.0*ATAN(1.0)
  DP = PI/72
  NXY = PI/DP
  D1 = 1/(FT1*FC1)
  D2 = 1/(FT2*FC2)
  D3 = (FC1-FT1)/(FC1*FT1)
  D4 = (FC2-FT2)/(FC2*FT2)
  D5 = 1/(F12*F12)
  AE = D1
  HE = D1/2
  BE = D2
  GE = D3/2
  FE = D4/2
  HHE = 1/(2*FT1*+T1)
  RC = 8.0*ATAN(1.0)/360.0
  T1 = 0.1E+8
  T2 = 0.1E+10
  AM = 0.0
  DM = 0.0
  READ(1,100) NC
  DO 99 NI = 1,NC
  READ(1,100) N
  DO 4 J = 1,3
  DO 4 K = 1,3
  A(J,K) = 0.0
  B(J,K) = 0.0
  D(J,K) = 0.0
4 CONTINUE
  TMA = 0.0
  TTH = 0.0
  DO 2 J = 1,N
  READ(1,104) F11(J),E22(J),ANU12(J),G12(J),RO(J),TH(J),THETAD(J)
  AMA(J) = RO(J)*TH(J)
  TMA = TMA+AMA(J)
  TTH = TTH + TH(J)
  ANU21(J)=ANU12(J)*E22(J)/E11(J)
  DENOM = 1.0 - ANU12(J)*ANU21(J)
  Q11(J) = E11(J)/DENOM
  Q12(J) = ANU21(J) * E11(J)/DENOM
  Q22(J) = F2/(J)/DENOM
  Q66(J) = G12(J)
2 CONTINUE
  H(1) = -TTH/2.0
  DO 1 J = 1,N
  IF(THETAD(J)) 13,10,14
10 Q11R(J) = Q11(J)
  Q12R(J) = Q12(J)
  Q16R(J) = 0 0

```

```

Q22B(J) = Q22(J)
Q26B(J) = 0.0
Q66B(J) = Q66(J)
THETAR(J) = THETAD(J)
GO TO 16
13 THETAR(J) = (360.0+THETAD(J))*RC
GO TO 15
14 THETAR(J) = THETAD(J)*RC
15 U1 = 0.125*(3.0*(Q11(J)+Q22(J))+2.0*Q12(J)+4.0*Q66(J))
U2 = 0.5*(Q11(J)-Q22(J))
U3 = 0.125*(Q11(J)+Q22(J)-2.0*Q12(J)-4.0*Q66(J))
U4 = 0.125*(Q11(J)+Q22(J)+6.0*Q12(J)-4.0*Q66(J))
U5 = 0.125*(Q11(J)+Q22(J)-2.0*Q12(J)+4.0*Q66(J))
A1 = U2*COS(2.0*THETAR(J))
A2 = U3*COS(4.0*THETAR(J))
A3 = 0.5*U2*SIN(2.0*THETAR(J))
A4 = U3*SIN(4.0*THETAR(J))
Q11B(J) = U1+A1+A2
Q12B(J) = U4-A2
Q16B(J) = -A3-A4
Q22B(J) = U1-A1+A2
Q26B(J) = -A3+A4
Q66B(J) = U5-A2
16 H(J+1) = H(J)+TH(J)
CTH = H(J+1)**3 - H(J)**3
A(1,1) = A(1,1)+Q11B(J)*TH(J)
A(1,2) = A(1,2)+Q12B(J)*TH(J)
A(1,3) = A(1,3)+Q16B(J)*TH(J)
A(2,2) = A(2,2)+Q22B(J)*TH(J)
A(2,3) = A(2,3)+Q26B(J)*TH(J)
A(3,3) = A(3,3)+Q66B(J)*TH(J)
IF(N.EQ.1) GO TO 21
STH = H(J+1)*H(J+1) - H(J)*H(J)
R1(J) = Q11B(J)*STH
R2(J) = Q12B(J)*STH
R3(J) = Q16B(J)*STH
R4(J) = Q22B(J)*STH
R5(J) = Q26B(J)*STH
R6(J) = Q66B(J)*STH
B(1,1) = B(1,1)+R1(J)
B(1,2) = B(1,2)+R2(J)
B(1,3) = B(1,3)+R3(J)
B(2,2) = B(2,2)+R4(J)
B(2,3) = B(2,3)+R5(J)
B(3,3) = B(3,3)+R6(J)
21 CONTINUE
D(1,1) = D(1,1)+Q11B(J)*CTH
D(1,2) = D(1,2)+Q12B(J)*CTH
D(1,3) = D(1,3)+Q16B(J)*CTH
D(2,2) = D(2,2)+Q22B(J)*CTH
D(2,3) = D(2,3)+Q26B(J)*CTH
D(3,3) = D(3,3)+Q66B(J)*CTH
1 CONTINUE
A(2,1) = A(1,2)
A(3,1) = A(1,3)
A(3,2) = A(2,3)
B(2,1) = B(1,2)
B(3,1) = B(1,3)
B(3,2) = B(2,3)
D(2,1) = D(1,2)
D(3,1) = D(1,3)
D(3,2) = D(2,3)
IF(N.EQ.1) GO TO 22
DO 70 J = 1,N
IF(ABS(R1(J)).GT.RM(1,1)) RM(1,1) = ABS(R1(J))
IF(ABS(R2(J)).GT.RM(1,2)) RM(1,2) = ABS(R2(J))

```



```

IF(ABS(R3(J)).GT.RM(1,3)) RM(1,3) = ABS(R3(J))
IF(ABS(R4(J)).GT.RM(2,2)) RM(2,2) = ABS(R4(J))
IF(ABS(R5(J)).GT.RM(2,3)) RM(2,3) = ABS(R5(J))
IF(ABS(R6(J)).GT.RM(3,3)) RM(3,3) = ABS(R6(J))
70 CONTINUE
RM(2,1) = RM(1,2)
RM(3,1) = RM(1,3)
RM(3,2) = RM(2,3)
22 DO 72 I = 1,3
DO 72 J = 1,3
IF(ABS(A(I,J)).GT.AM) AM = ABS(A(I,J))
IF(ABS(D(I,J)).GT.DM) DM = ABS(D(I,J))
72 CONTINUE
DO 71 I = 1,3
DO 71 J = 1,3
IF(A(I,J)) 80,81,79
79 IF(AM/A(I,J).GT.T2) A(I,J) = 0.0
GO TO 81
80 IF(AM/ABS(A(I,J)).GT.T2) A(I,J) = 0.0
81 IF(N.EQ.1) GO TO 83
IF(R(I,J)) 82,83,85
85 IF(RM(I,J)/R(I,J).GT.T1) B(I,J) = 0.0
GO TO 83
82 IF(RM(I,J)/ABS(B(I,J)).GT.T1) B(I,J) = 0.0
83 IF(D(I,J)) 84,71,86
86 IF(DM/D(I,J).GT.T2) D(I,J) = 0.0
GO TO 71
84 IF(DM/ABS(D(I,J)).GT.T2) D(I,J) = 0.0
71 CONTINUE
DO 5 J = 1,3
DO 5 K = 1,3
D(J,K) = D(J,K)/3.0
B(J,K) = B(J,K)*0.5
C(J,K) = A(J,K)
C(J,K+3) = B(J,K)
C(J+3,K) = B(J,K)
C(J+3,K+3) = D(J,K)
5 CONTINUE
WRITE(2,112)
DO 3 J = 1,N
WRITE(2,116) J,E11(J),E22(J),ANU12(J),ANU21(J),G12(J),RO(J),TH(J),
1THFTAD(J)
3 CONTINUE
WRITE(2,121) TTH
WRITE(2,120) TMA
DO 20 I = 1,3
DO 20 J = 1,3
IF(B(I,J)) 51,20,51
20 CONTINUE
IF(A(1,3).EQ.0.0.AND.A(2,3).EQ.0.0) GO TO 50
GO TO 51
50 A1 = A(1,2)*A(1,2)
EXX = (A(1,1)-A1/A(2,2))/TTH
EYY = (A(2,2)-A1/A(1,1))/TTH
GXY = A(3,3)/TTH
ANUXY = A(1,2)/A(2,2)
ANUYX = A(1,2)/A(1,1)
WRITE(2,110) EXX
WRITE(2,105) EYY
WRITE(2,115) GXY
WRITE(2,111) ANUXY
WRITE(2,113) ANUYX
51 CONTINUE
CALL FMOVE(A,AA,9)
CALL POSDEF MATINV(AA,9)
CALL MUIT(AA,3,,S,1,ES)

```

```

CALL WRITE (ES,3,1,5HSTRXY)
ES(3) = FS(3)/2
DO 99 J = 1,1
FF1 = E11(1)
FF2 = E22(1)
FF3 = G12(1)
U(J) = THETAR(J)
SQ = SIN(U(J))
CQ = COS(U(J))
CCQ = CQ*CQ
SSQ = SQ*SQ
SCQ = SQ*CQ
T(1,1) = CCQ
T(1,2) = SSQ
T(1,3) = 2*SCQ
T(2,1) = T(1,2)
T(2,2) = T(1,1)
T(2,3) = -2*SCQ
T(3,1) = -SCQ
T(3,2) = SCQ
T(3,3) = CCQ-SSQ
Q(1,1) = Q11(J)
Q(1,2) = Q12(J)
Q(1,3) = 0
Q(2,1) = Q(1,2)
Q(2,2) = Q22(J)
Q(2,3) = 0
Q(3,1) = 0
Q(3,2) = 0
Q(3,3) = Q66(J)
CALL WRITE(T,3,3,5HT      )
CALL MUIT(T,3,3,ES,1,EN)
EN(3) = FN(3)*2
CALL WRITE(EN,3,1,5HSTR12)
CALL MUIT(Q,3,3,EN,1,SN)
CALL WRITE(SN,3,1,5HSIG12)
CE = D5*SN(3)*SN(3)-1.0
CZ = CE
WRITE(2,102) D1,D2,D3,D4,D5,AE,HE,BE,GE,FE,CE,DS
CALL FAILURE STRESS
CALL HILL STRESS
CALL MAX STRAIN
CALL MAX STRESS
99  CONTINUE
STOP
90  FORMAT(6(E0.0),F0.0)
102 FORMAT(1X,11(E9.2,1X),E9.2)
100  FORMAT(10)
101  FORMAT(1H0,6(F14.10,2X))
104  FORMAT(2E0.0,F0.0,3E0.0,F0.0)
112  FORMAT(1H1,6HLAMINA,5X,3HE11,11X,3HE22,11X,4HNU12,10X,4HNU21,10X,3
1HG12,9X,7HDENSITY,8X,9HTHICKNESS,7X,5HANGLE)
116  FORMAT(3X,13,1X,8(F12.5,2X))
120  FORMAT(1H0,61HTOTAL MASS/UNIT SURFACE AREA (I.E.DENSITY*TOTAL THIC
1KNNESS) = ,E17.10)
121  FORMAT(1H0,27HLAMINATE TOTAL THICKNESS = ,F12.10)
110  FORMAT(1H0,'LAMINATE LONGITUDINAL STIFFNESS, EXX = ',E17.10)
105  FORMAT(1H0,'LAMINATE TRANSVERSE STIFFNESS, EYY = ',E17.10)
115  FORMAT(1H0,'LAMINATE SHEAR STIFFNESS, GXY = ',E17.10)
111  FORMAT(1H0,'LAMINATE PRINCIPAL POISSONS RATIO, NUXY = ',F13.10)
113  FORMAT(1H0,'LAMINATE TRANSVERSE POISSONS RATIO, NUYX = ',F13.10)
END

SUBROUTINE MAX STRAIN
DIMENSION FN(3),S(3),SN(3)

```

```

COMMON/R7/FN/R8/EE1,EE2,EE3/B4/SN,S/B1/FT1,FC1,FT2,FC2,F12
F1 = ABS(EN(1))
F2 = ABS(EN(2))
F3 = ABS(EN(3))
ET1 = FY1/EE1
EC1 = FC1/EF1
ET2 = FY2/EE2
FC2 = FC2/EE2
E12 = F12/EE3
EM = -0.1F+50
T1 = 0.1E+10
T2 = 0.1F-20
RL = 0.1F+50
IF(E1.GT.EM) EM = EN(1)
IF(F2.GT.EM) EM = EN(2)
IF(F3.GT.EM) EM = EN(3)
IF(E1-T2) 12,12,13
13 IF(FM/E1.GT.T1) EN(1) = 0.0
12 IF(F2-T2) 14,14,15
15 IF(FM/E2.GT.T1) EN(2) = 0.0
14 IF(F3-T2) 16,16,17
17 IF(FM/E3.GT.T1) EN(3) = 0.0
16 CONTINUE
CALL WRITE(EN,3,1,5HSTR12)
IF(FN(1)) 1,2,3
1 R1 = EC1/E1
GO TO 7
2 R1 = RL
GO TO 7
3 R1 = ET1/E1
7 CONTINUE
IF(EN(2)) 4,5,6
4 R2 = EC2/E2
GO TO 8
5 R2 = RL
GO TO 8
6 R2 = ET2/E2
8 CONTINUE
IF(FN(3)) 9,10,9
9 R3 = E12/F3
GO TO 11
10 R3 = RL
11 CONTINUE
IF(R1.LT.RL) RL = R1
IF(R2.LT.RL) RL = R2
IF(R3.LT.RL) RL = R3
WRITE(2,102) A1,A2,AS1,AS2,AS3,R1,R2,R3,RL,SM
102 FORMAT(1X,12(E9.2,1X))
IF(RL.EQ.R1) GO TO 20
IF(RL.EQ.R2) GO TO 21
GO TO 22
20 CONTINUE
SX = R1*S(1)
24 CONTINUE
WRITE(2,390) SX
390 FORMAT(1X,'FAILURE AT SX = ',E17.10)
GO TO 100
21 SX = R2*S(1)
GO TO 24
22 CONTINUE
SX = R3*S(1)
WRITE(2,391) SX
391 FORMAT(1X,'SHEAR FAILURE AT SX = ',E17.10)
100 CONTINUE
RETURN
END

```

```

SUBROUTINE MAX STRESS
DIMENSION SN(3),S(3)
COMMON/R4/SN,S/R1/FT1,FC1,FT2,FC2,F12
R1 = 0.1E+50
T1 = 0.1E-12
T2 = 0.1E+10
SM = -0.1E+50
AS1 = ABS(SN(1))
AS2 = ABS(SN(2))
AS3 = ABS(SN(3))
IF(AS1.GE.SM) SM = AS1
IF(AS2.GE.SM) SM = AS2
IF(AS3.GE.SM) SM = AS3
IF(SM-AS1.GE.T2) SN(1) = 0.0
IF(SM-AS2.GE.T2) SN(2) = 0.0
IF(SM-AS3.GE.T2) SN(3) = 0.0
CALL WRITE(SN,3,1,5HSIG12)
IF(SN(1)) 1,2,3
1  A1 = FC1
   R1 = A1/AS1
   GO TO 7
2  R1 = RL
   GO TO 7
3  A1 = FT1
   R1 = A1/AS1
7  CONTINUE
   IF(SN(2)) 4,5,6
4  A2 = FC2
   R2 = A2/AS2
   GO TO 8
5  R2 = RL
   GO TO 8
6  A2 = FT2
   R2 = A2/AS2
8  CONTINUE
   IF(SN(3)) 9,10,9
9  R3 = F12/AS3
   GO TO 11
10 R3 = RL
11 CONTINUE
102 WRITE(2,102) A1,A2,AS1,AS2,AS3,R1,R2,R3,RL,SM
    FORMAT(1X,12(E9.2,1X))
    IF(R1.LT.RL) RL = R1
    IF(R2.LT.RL) RL = R2
    IF(R3.LT.RL) RL = R3
    IF(R1.EQ.R1) GO TO 20
    IF(R1.EQ.R2) GO TO 21
    GO TO 22
20 CONTINUE
   SX = R1*S(1)
24 CONTINUE
   WRITE(2,390) SX
390 FORMAT(1X,'FAILURE AT SX = ',E17.10)
   GO TO 100
21 SX = R2*S(1)
   GO TO 24
22 CONTINUE
   SX = R3*S(1)
   WRITE(2,391) SX
391 FORMAT(1X,'SHEAR FAILURE AT SX = ',E17.10)
100 CONTINUE
    RETURN
    END

```

```

SUBROUTINE FAILURE STRESS
DIMENSION SN(3),S(3)
COMMON/B4/SN,S/B2/AE,HE,BE,GE,FE,CE,HAE,HNE,HBE/B6/D5
1/B1/FT1,FC1,FT2,FC2,F12
CALL WRITE(S,3,1,5HSIGXY)
CALL WRITE(SN,3,1,5HSIG12)
T1 = 0.1E-20
IF(ABS(SN(1)).LE.T1.AND.ABS(SN(2)).LE.T1) GO TO 10
3 SL = SN(2)/SN(1)
  SL1 = SN(3)/SN(1)
  QB = -(GE+FE*SL)
  Q1 = AE-2*HE*SL+BE*SL*SL+D5*SL1*SL1
  Q2 = QB*QB+Q1
  IF(Q2) 1,1,2
1  WRITE(2,99)
99 FORMAT(1X,'COMPLEX ROOTS TO QUADRATIC')
  GO TO 322
2  QR = SQRT(Q2)
  IF(SN(1)) 310,310,311
310 SM1 = (QB-QR)/Q1
  GO TO 312
311 SM1 = (QB+QR)/Q1
312 CONTINUE
  RA = SM1/SN(1)
  SMS = RA*SN(3)
  IF(ABS(SMS)-F12) 320,320,321
321 CONTINUE
  RA1 = F12/ABS(SN(3))
  SX = RA1*S(1)
  WRITE(2,390) SX
390 FORMAT(1X,'SHEAR FAILURE AT SX = ',E17.10)
  GO TO 322
320 CONTINUE
  SX = RA*S(1)
  WRITE(2,391) SX
391 FORMAT(1X,'FAILURE AT SX = ',E17.10)
102 FORMAT(1X,11(E9.2,1X),E9.2)
322 CONTINUE
  WRITE(2,102) SL,QB,Q1,QR,SM1,RA,SMS,RA1,SX
10 RETURN
END

```

```

SUBROUTINE HILL STRESS
DIMENSION SN(3),S(3)
COMMON/B4/SN,S/B2/AE,HE,BE,GE,FE,CE,HAE,HNE,HBE/B6/D5
1/B1/FT1,FC1,FT2,FC2,F12
CALL WRITE(S,3,1,5HSIGXY)
CALL WRITE(SN,3,1,5HSIG12)
T1 = 0.1E-20
IF(ABS(SN(1)).LE.T1.AND.ABS(SN(2)).LE.T1) GO TO 21
3 SL = SN(2)/SN(1)
  SL1 = SN(3)/SN(1)
  IF(SN(1)) 10,10,11
10 IF(SN(2)) 12,12,13
12 PA = 1/(FC1*FC1)
  PB = 1/(FC2*FC2)
  PH = 1/(2*FC1*FC1)
  GO TO 20
13 PA = 1/(FC1*FC1)
  PB = 1/(FT2*FT2)
  PH = 1/(2*FC1*FC1)
  GO TO 20
11 IF(SN(2)) 14,14,15
14 PA = 1/(FT1*FT1)

```

```

PB = 1/(FC1*FC1)
PH = 1/(2*FT1*FT1)
GO TO 20
1 PA = 1/(FT1*FT1)
PB = 1/(FT2*FT2)
PH = 1/(2*FT1*FT1)
20 CONTINUE
Q1 = PA-2*PH*SL+PB*SL*SL+D5*SL1*SL1
IF(Q1) 1,1,2
1 WRITE(2,99)
99 FORMAT(1X,'COMPLEX ROOTS TO QUADRATIC')
GO TO 322
2 QR = SQRT(Q1)
IF(SN(1)) 310,310,311
310 SM1 = -QR/Q1
GO TO 312
311 SM1 = QR/Q1
312 CONTINUE
RA = SM1/SN(1)
SMS = RA*SN(3)
IF(ABS(SMS)-F12) 320,320,321
321 CONTINUE
RA1 = F12/ABS(SN(3))
SX = RA1*S(1)
WRITE(2,390) SX
390 FORMAT(1X,'SHEAR FAILURE AT SX = ',E17.10)
GO TO 322
320 CONTINUE
SX = RA*S(1)
WRITE(2,391) SX
391 FORMAT(1X,'FAILURE AT SX = ',E17.10)
102 FORMAT(1X,11(E9.2,1X),E9.2)
322 CONTINUE
WRITE(2,102) SL,Q6,Q1,QR,SM1,RA,SMS,RA1,SX
21 RETURN
END

```

```

SUBROUTINE POSDEF MATINV(A,MAMA)
C * * * * * INV 0000
C * * * * * INV 0010
C THE SUBROUTINE FINDS THE INVERSE OF THE MA BY MA SYMMETRIC POSITIVE INV 0020
C DEFINITE MATRIX [A]. THE SUBROUTINE REQUIRES: INV 0030
C THE REAL ARRAY A(MA,MA) CONTAINING THE COMPLETE MATRIX [A]. INV 0040
C A IS OVERWRITTEN BY ITS INVERSE. (MAMA=MA*MA) INV 0050
C * * * * * INV 0060
REAL A(MAMA) INV 0070
INTEGER ROW,COL INV 0080
MA=0.1+SQRT(1.0*MAMA) INV 0090
J1=MAMA-MA+1 INV 0100
J2=0 INV 0110
DO 1 COL=1,J1,MA INV 0120
J2=J2+1 INV 0130
DO 1 ROW=1,MA INV 0140
J3=ROW+COL-1 INV 0150
R=0.0 INV 0160
IF(J2.E0.1.OR.ROW-J2.LT.0)GOTO4 INV 0170
J4=ROW INV 0180
DO 2 M=1,J2-1 INV 0190
B=B+A(J4)*A(J2+J4-ROW) INV 0200
2 J4=J4+MA INV 0210
4 IF(ROW-J2)1,3,0 INV 0220
A(J3)=(A(J3)-B)/A(COL+J2-1) INV 0230
GOTO1 INV 0240
3 A(J3)=SQRT(A(J3)-B) INV 0250
1 CONTINUE INV 0260
J2=0 INV 0270

```

```

DO 5 COL=1,J1,MA
J2=J2+1
J5=-MA
DO 5 ROW=1,MA
J3=ROW+COL-1
J5=J5+MA
B=0.0
IF(ROW-J2.LE.0)GOTO6
J4=J3
DO 7 M=J2,ROW-1
B=B+A(J4)*A(COL+M-1)
7 J4=J4+MA
6 IF(ROW-J2)5,8,0
A(J3)=-B/A(ROW+J5)
GOTO5
8 A(J3)=1.0/A(COL+J2-1)
5 CONTINUE
J2=0
DO 9 COL=1,J1,MA
J4=0
J2=J2+1
DO 9 ROW=1,J1,MA
J4=J4+1
B=0.0
IF(J4-J2)11,0,0
DO 10 M=J4,MA
10 B=B+A(ROW+M-1)*A(COL+M-1)
GOTO12
11 A(COL+J4-1)=A(ROW+J2-1)
GOTO9
12 A(COL+J4-1)=B
9 CONTINUE
RETURN
END
SUBROUTINE WRITE(AM,I,J,DUMMY)
DIMENSION AM(I,J)
WRITE(2,200) DUMMY
200 FORMAT(1H0,7H MATRIX,2X,A5)
111 FORMAT(1X,6(E17.10,2X))
DO 1 K = 1,I
WRITE(2,111) (AM(K,L),L = 1,J)
1 CONTINUE
RETURN
END

SUBROUTINE MULT(A,I,J,B,K,C)
DIMENSION A(I,J),B(J,K),C(I,K)
DO 1 L = 1,I
DO 1 M = 1,K
C(L,M) = 0.0
DO 1 N = 1,J
C(L,M) = C(L,M)+A(L,N)*B(N,M)
1 CONTINUE
RETURN
END
SUBROUTINE SCHMULT(A,I,J,S)
DIMENSION A(I,J)
DO 1 K = 1,I
DO 1 L = 1,J
A(K,L) = A(K,L)+S
1 CONTINUE
RETURN
END

```

```

INV 0280
INV 0290
INV 0300
INV 0310
INV 0320
INV 0330
INV 0340
INV 0350
INV 0360
INV 0370
INV 0380
INV 0390
INV 0400
INV 0410
INV 0420
INV 0430
INV 0440
INV 0450
INV 0460
INV 0470
INV 0480
INV 0490
INV 0500
INV 0510
INV 0520
INV 0530
INV 0540
INV 0550
INV 0560
INV 0570
INV 0580
INV 0590
INV 0600
INV 0610

```

```
SUBROUTINE SUB(A,I,J,B,C)
DIMENSION A(I,J),B(I,J),C(I,J)
DO 1 K = 1,I
DO 1 L = 1,J
C(K,I) = A(K,I)-B(K,I)
1 CONTINUE
RETURN
END
FINISH
```



## Program listing

## Angle-ply-theory coefficient

```

0010          MASTER NON LIN LAM
0011          E1 = 0.165 E+12
0012          E2 = 0.93 E+10
0013          Q = 0.33
0014          G = 0.49 E+10
0015          AL = 0.7853981633
0016          T = 0.8726646259 E-01
0017          DT = 0.8726646259 E-01
0018          3      S = SIN(T)
0019          C = COS(T)
0020          SC = S*C
0021          CC = C*C
0022          SS = S*S
0023          A = E2*(1+Q)/(Q*E2+E1)
0024          B = (Q*E2+E1)/(E1*E2)
0025          D = (1+Q)/E1
0026          A1 = (2*SC)/(SS+A*CC)
0027          A2 = CC*(CC-SS)/(2*B*SS*SC+2*D*CC*SC)
0028          B1 = 2*SC/(SS/A+CC)
0029          B2 = -SS*(CC-SS)/(2*B*SS*SC+2*D*CC*SC)
0030          A3 = 1/E1*(A1-Q*B1)
0031          A4 = 1/E1*(A2-Q*B2)
0032          B3 = B1/E2-Q*A1/E1
0033          B4 = B2/E2-Q*A2/E1
0034          A5 = A3*CC+B3*SS
0035          A6 = A4*CC+B4*SS+SC
0036          B5 = A3*SS+B3*CC
0037          B6 = A4*SS+B4*CC-SC
0038          SX = A5*G+A6
0039          R = (B5*G+B6)/SX
0040          A7 = A1*CC+B1*SS+2*SC
0041          A8 = A2*CC+B2*SS
0042          PX = A7*G+A8
0043          EX = PX/SX
0044          WRITE(2,10)SX,R,PX,EX,A5,A6,A7,A8
0045          WRITE(2,10)A1,A2,B1,B2,A3,A4,B3,B4
0046          10      FORMAT(8(1X,E14.6))
0047          IF(AL-T)1,1,2
0048          2      T = T+DT
0049          GO TO 3
0050          1      STOP
0051          END

```

END OF SEGMENT, LENGTH 274, NAME NONLINLAM

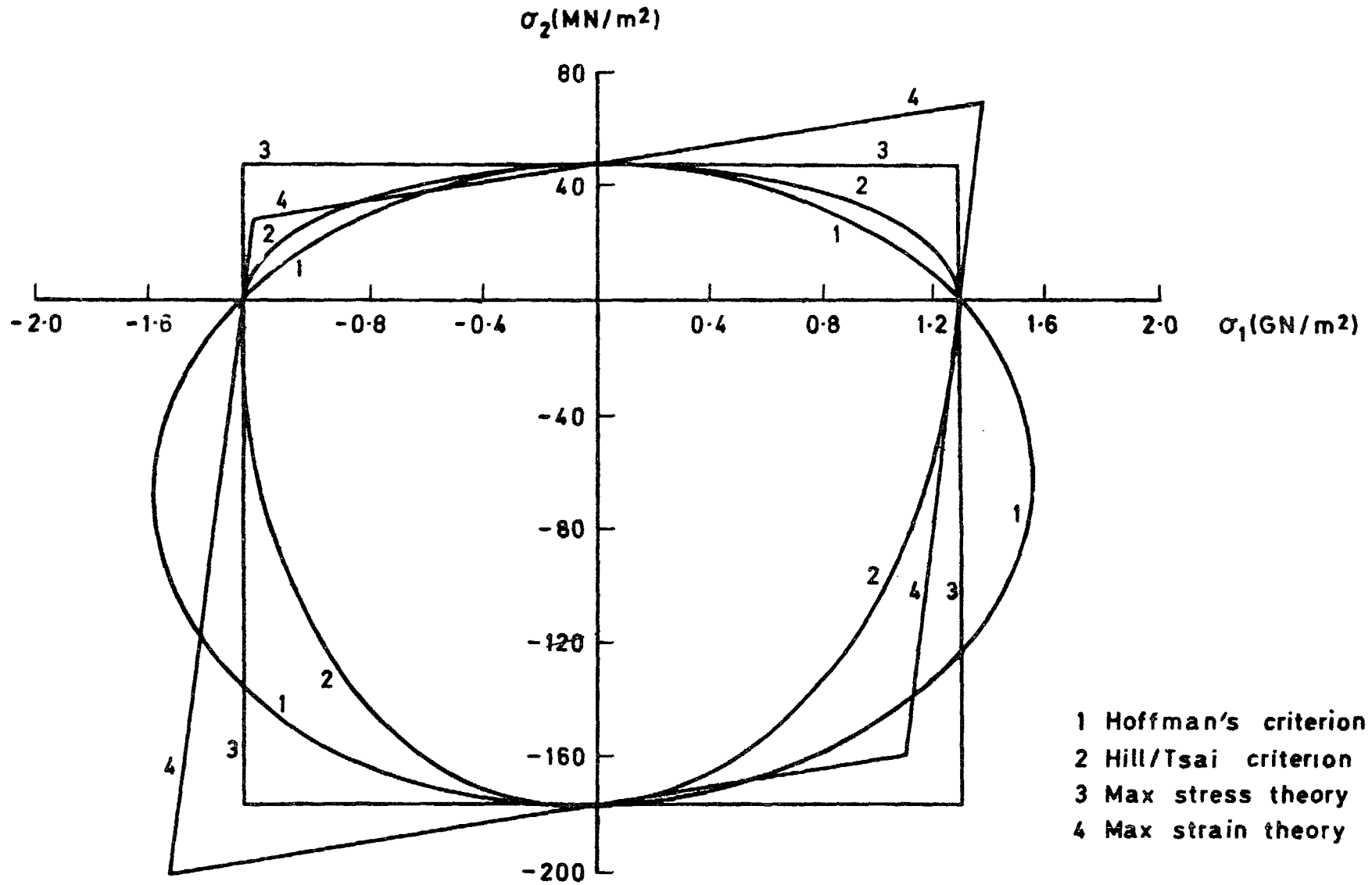


Fig 1 Four failure theories as applied to a high strength (HT-S) unidirectional laminate

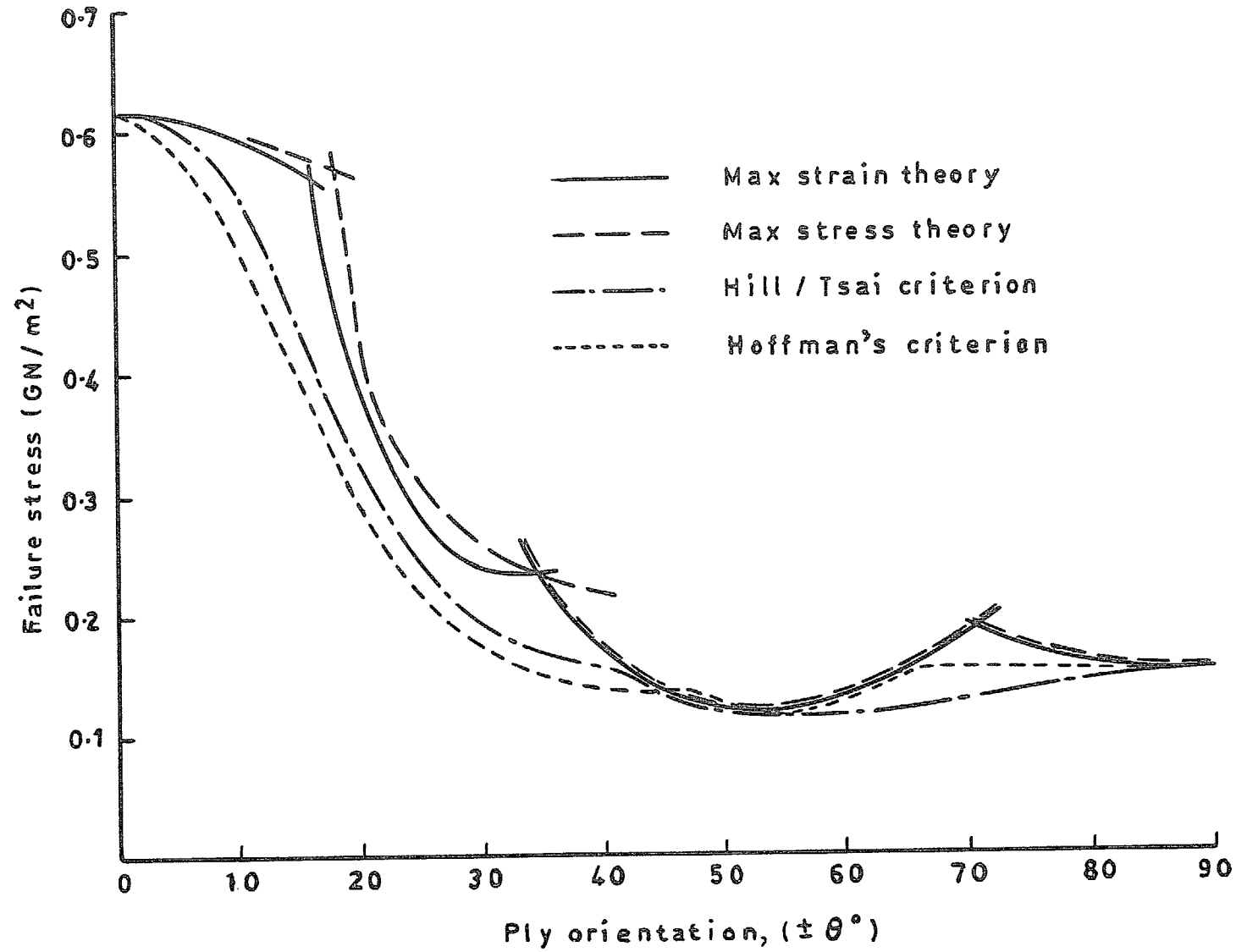


Fig 2 Variation of compressive strength with orientation according to four theories for high modulus (HM-S) angle-ply laminates

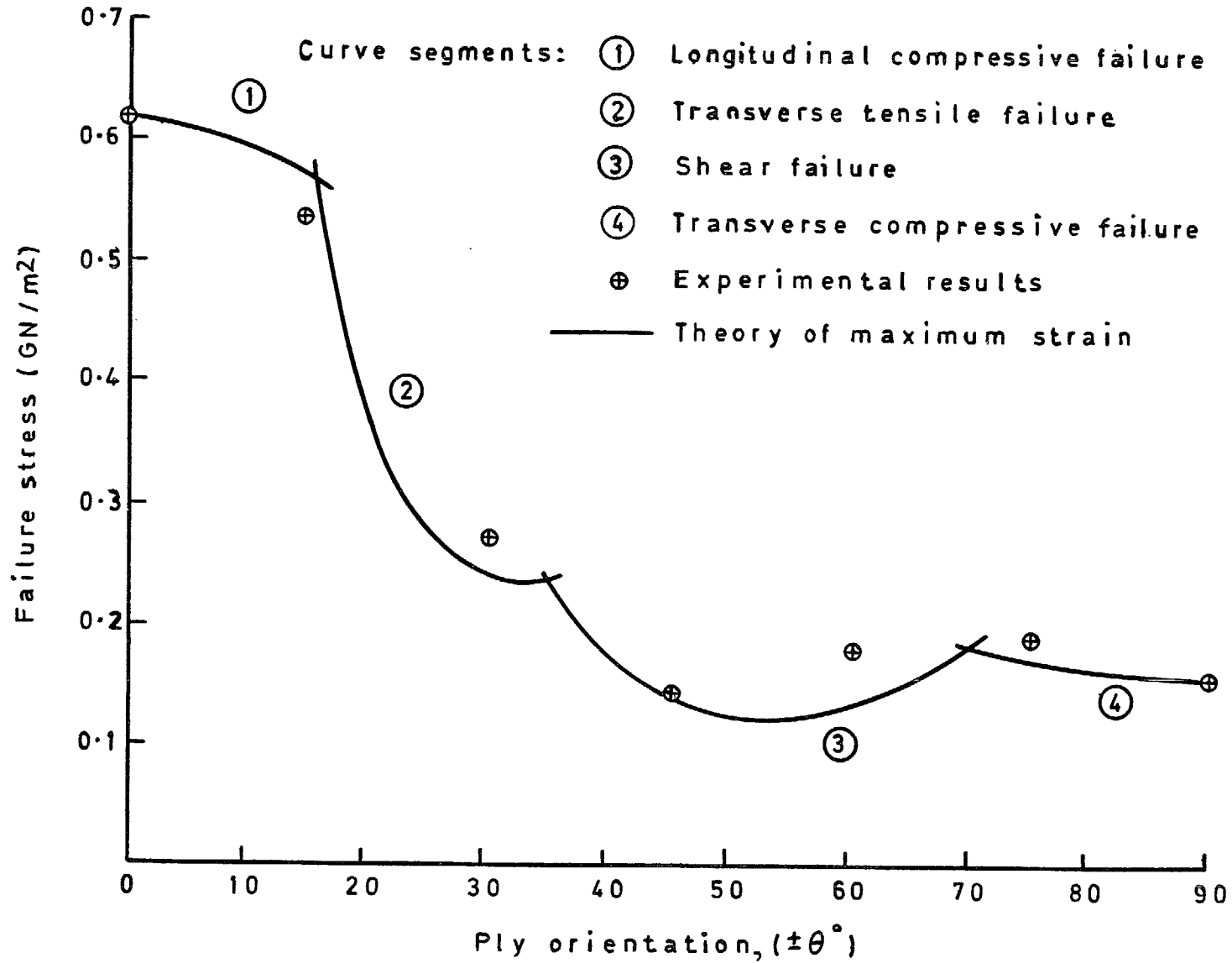


Fig 3 Comparison between experiment and theory of max strain for compressive strength for high modulus (HM-S) angle-ply laminates

Fig 4

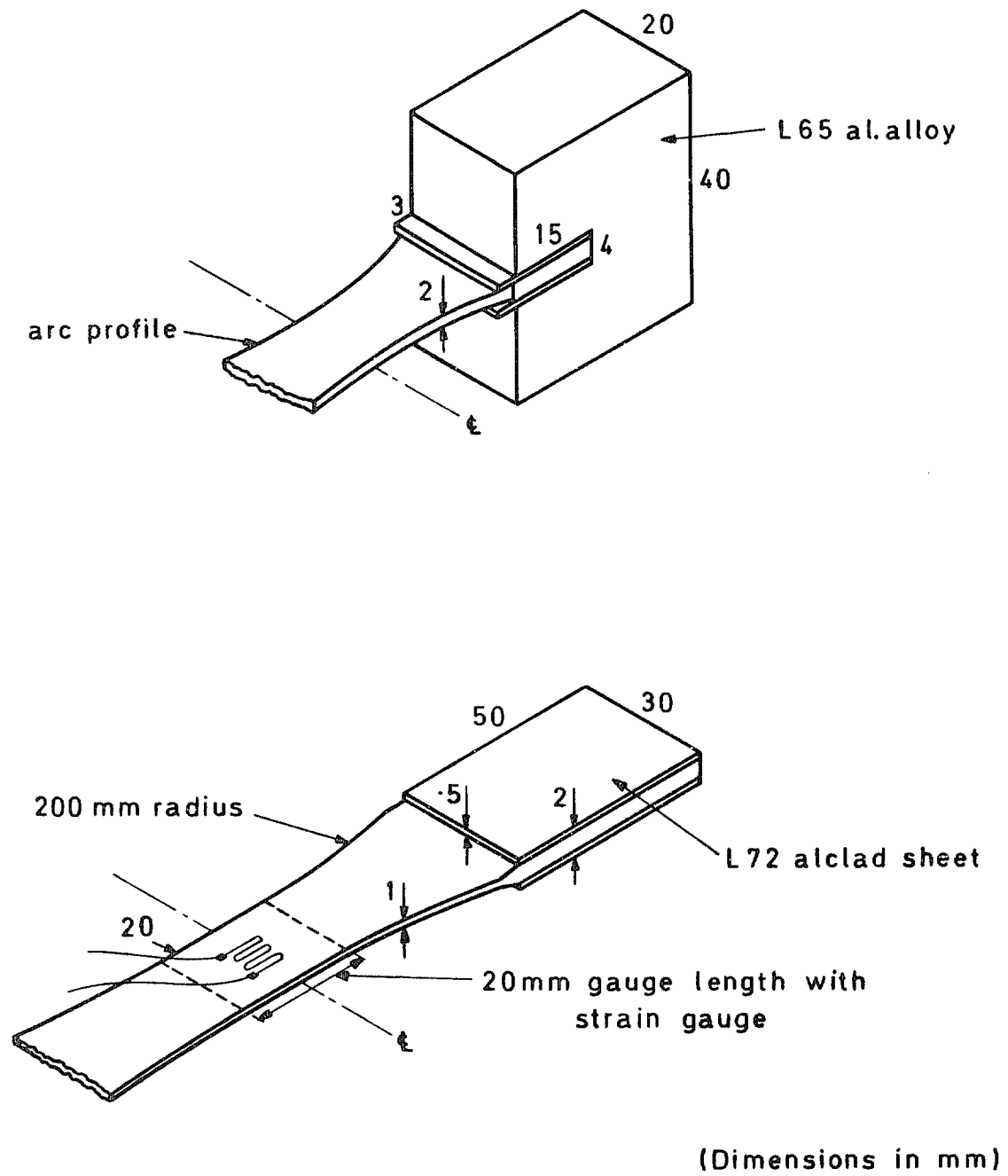


Fig 4 Compressive and tensile specimen design

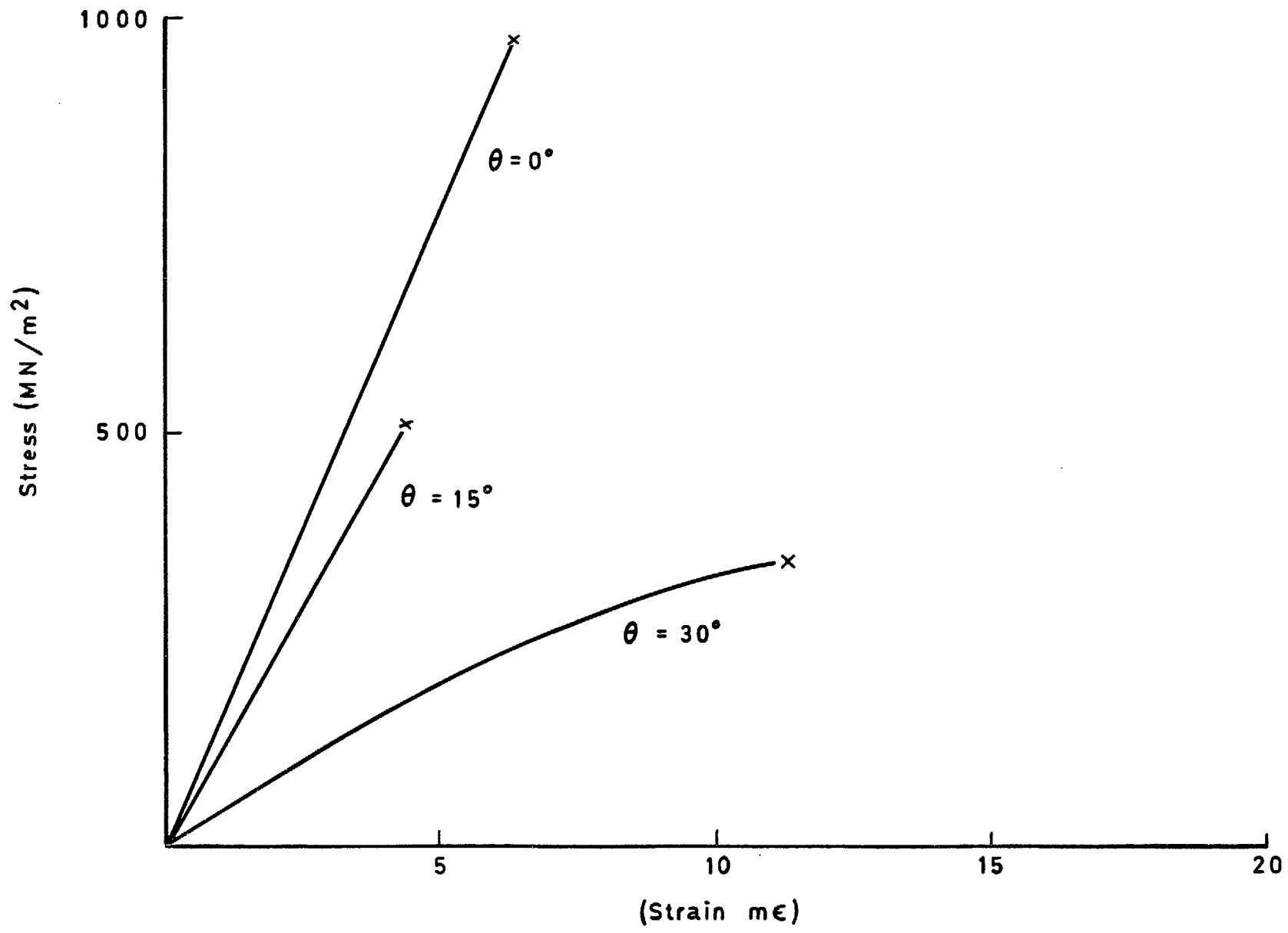


Fig 5 Typical HT-S angle-ply stress/strain curves for various ply orientations

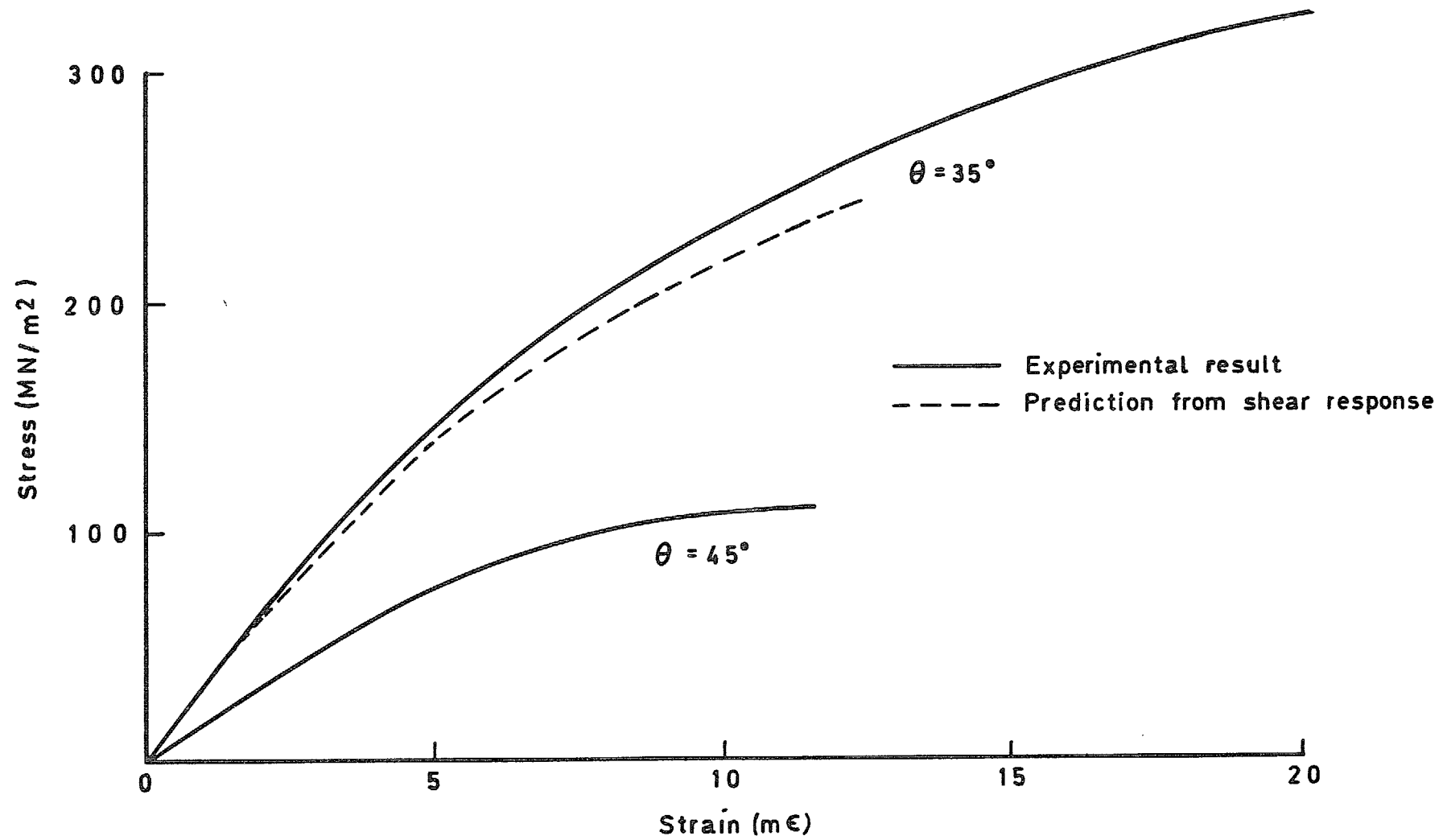


Fig 6 Typical HT-S angle-ply stress/strain curves, for  $\theta = 35^\circ$  and  $\theta = 45^\circ$

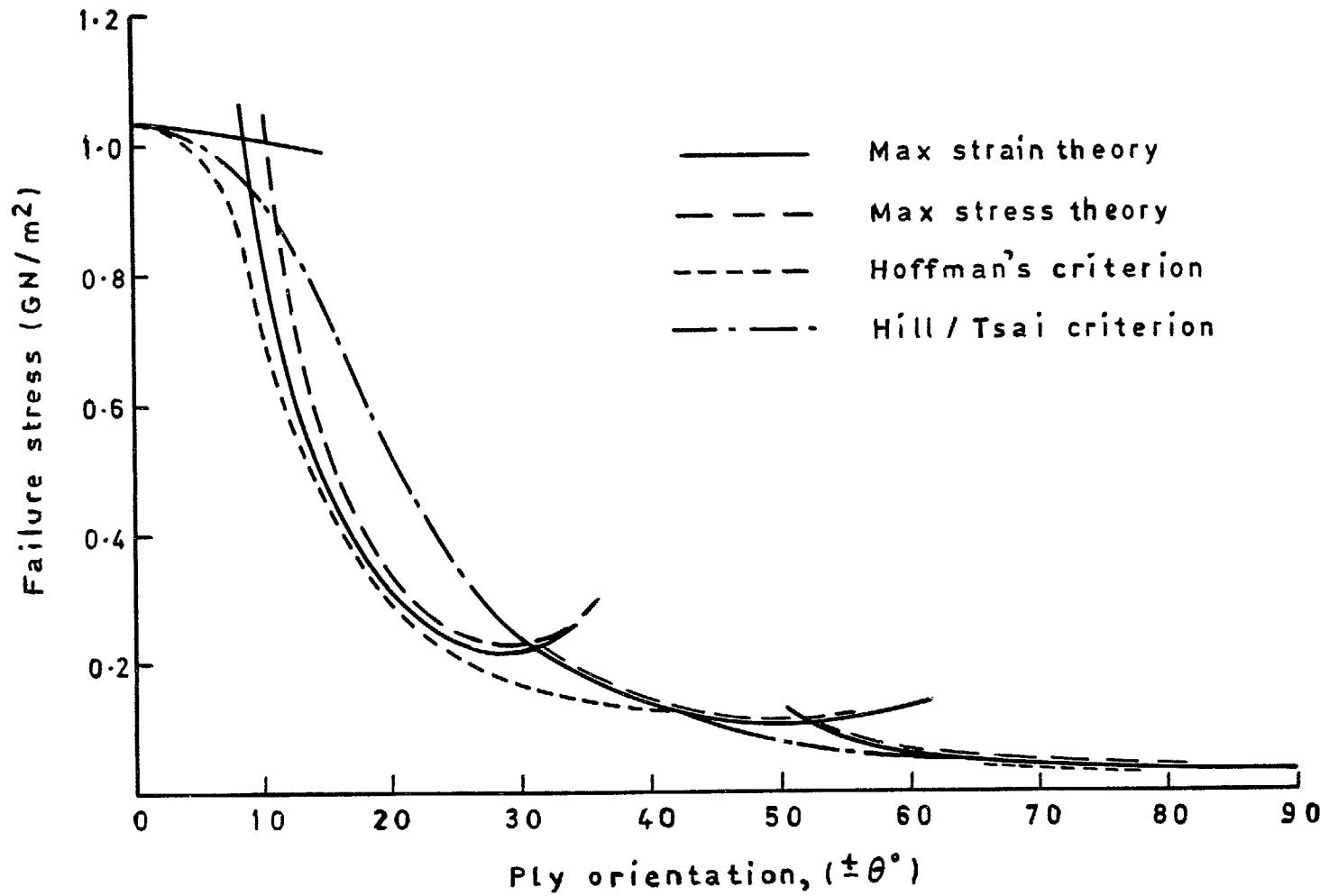


Fig 7 Comparison between theories of failure for tensile strength of angle-ply HT-S laminates



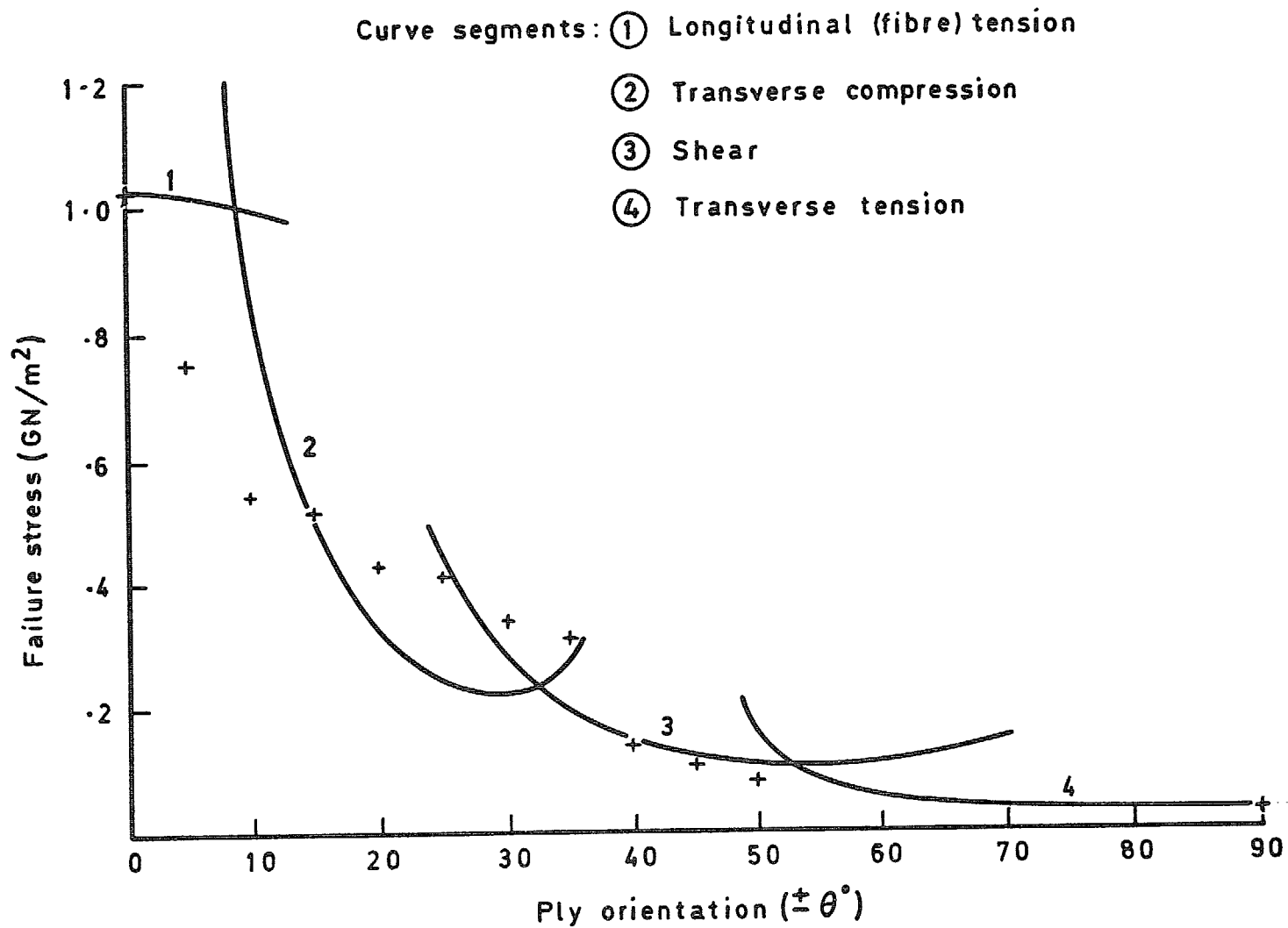


Fig 8 Comparison between experiment and theory of max strain for tensile strength of HT-S angle-ply laminates

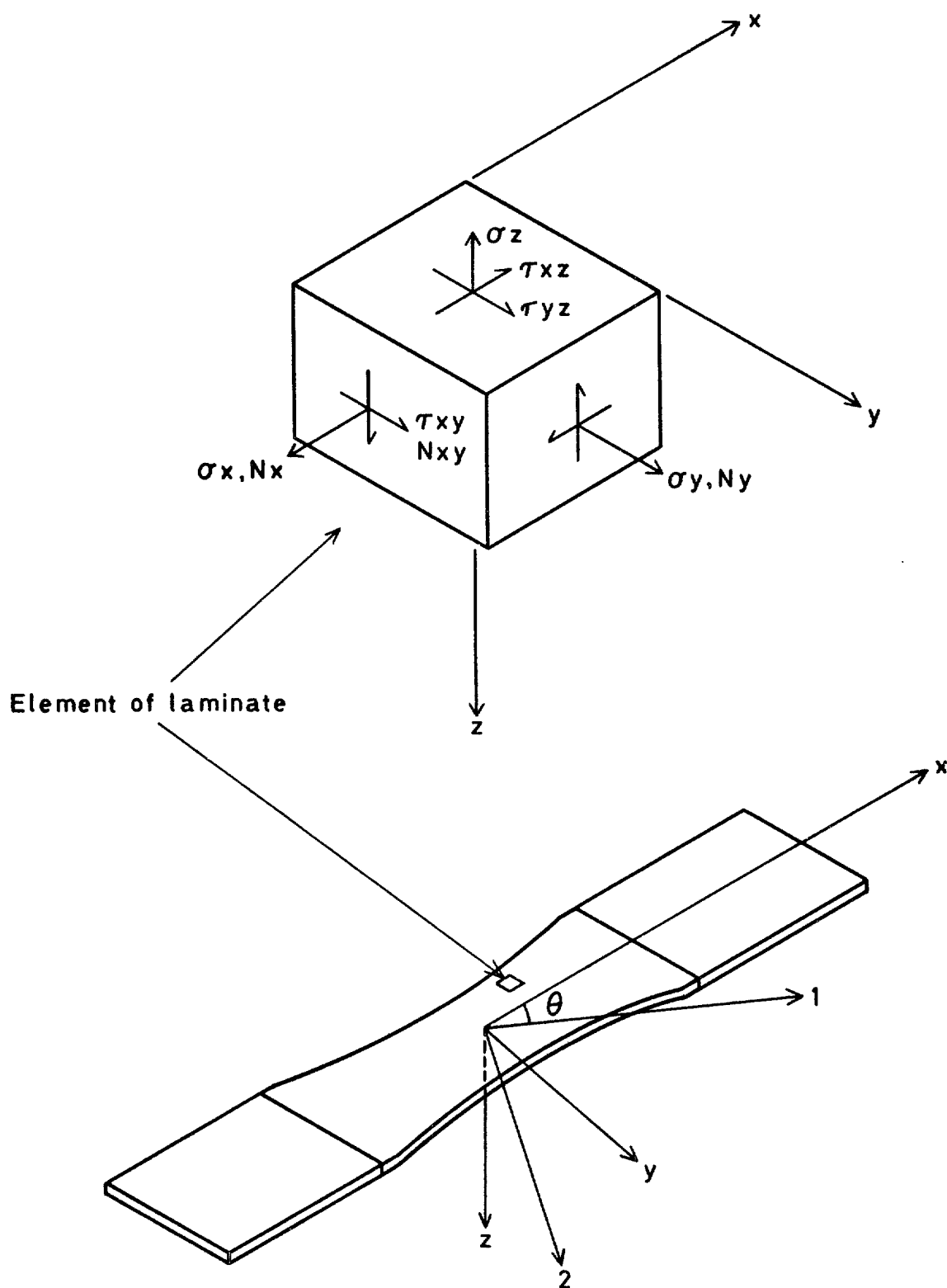


Fig 9 Notation and sign convention for laminate stresses

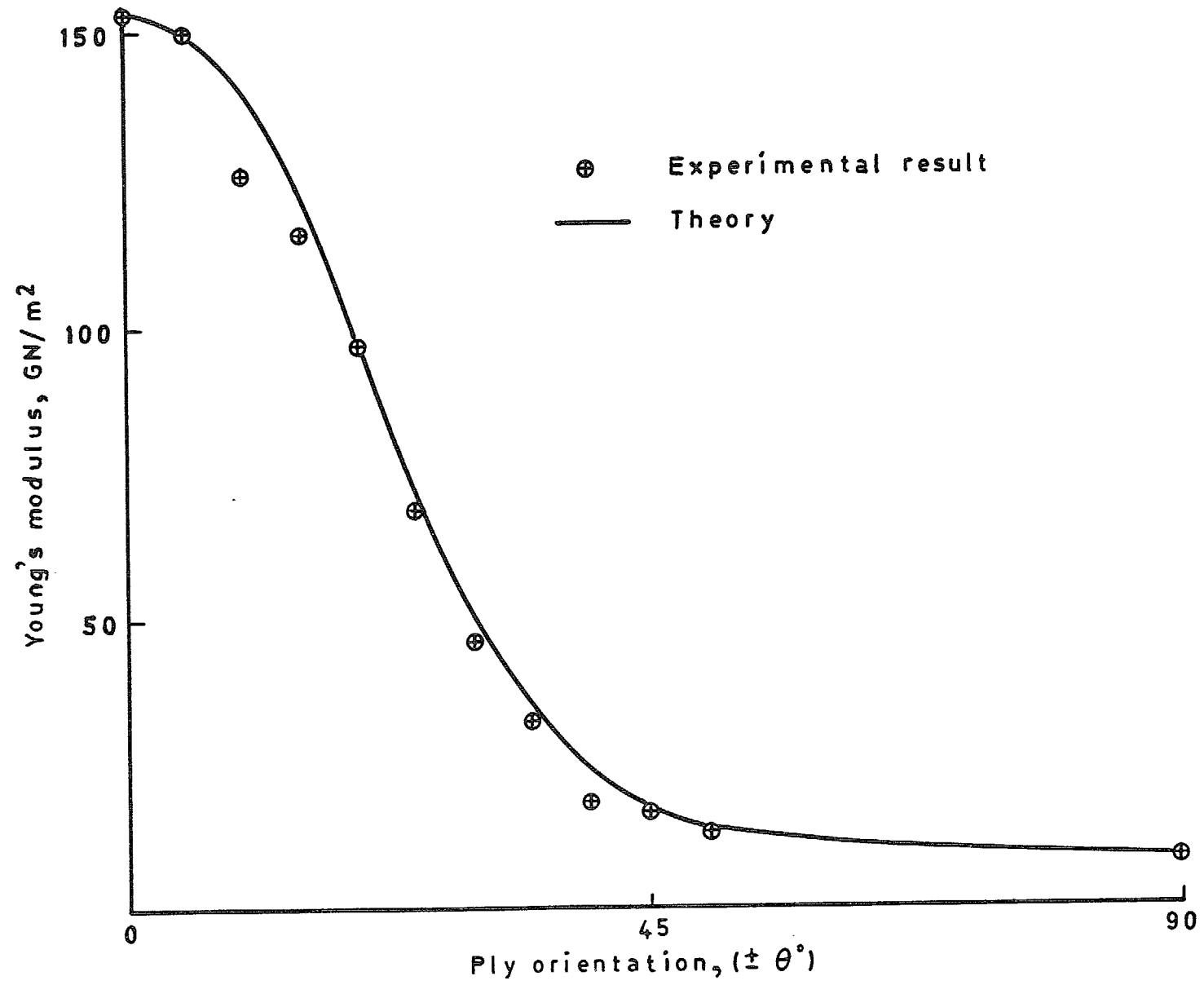


Fig 10 Variation of Young's modulus with orientation for high strength HT-S angle-ply laminates

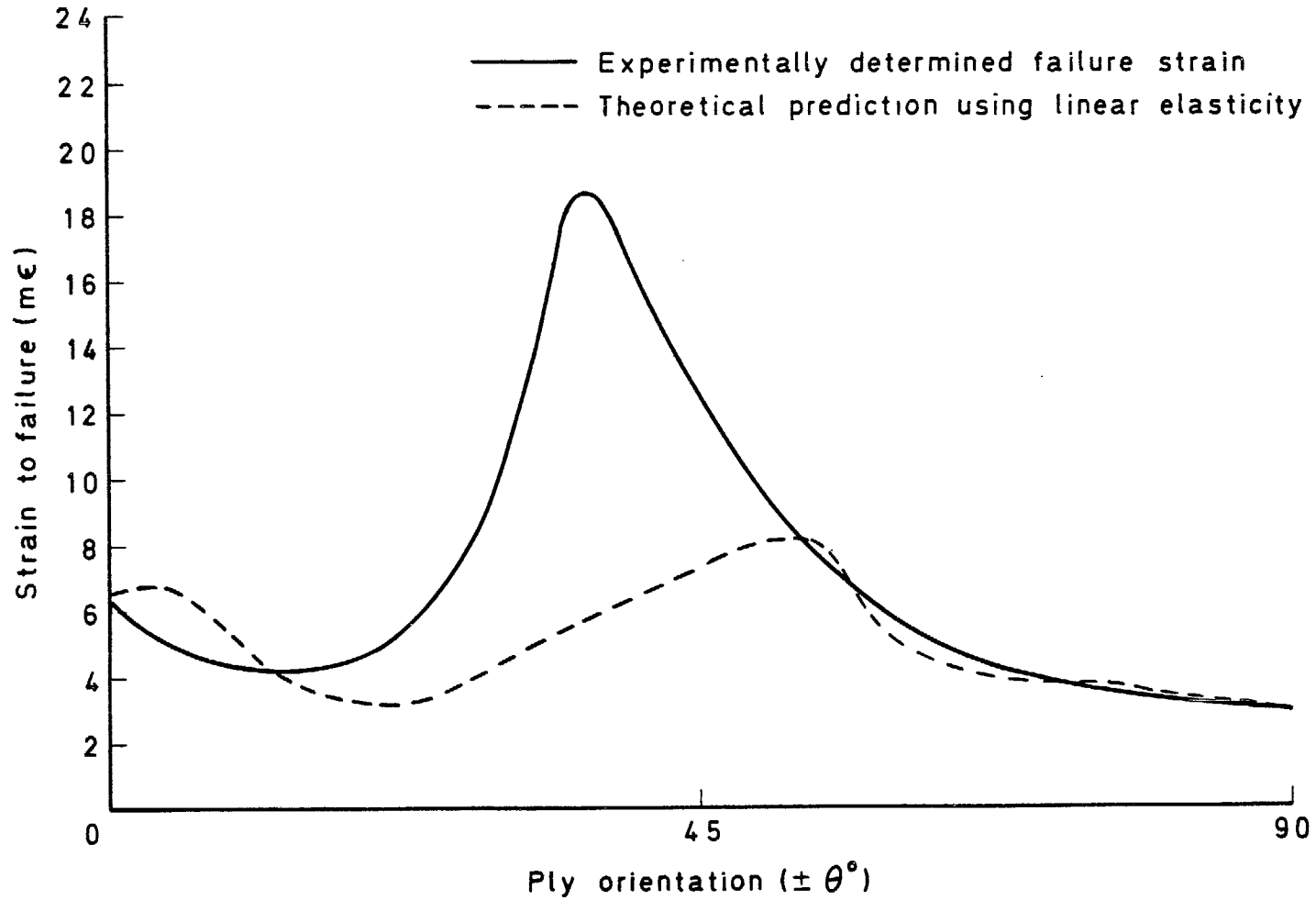


Fig 11 Comparison between experimental and theoretical failure strain for high strength (HT-S) angle-ply laminates

Fig 12

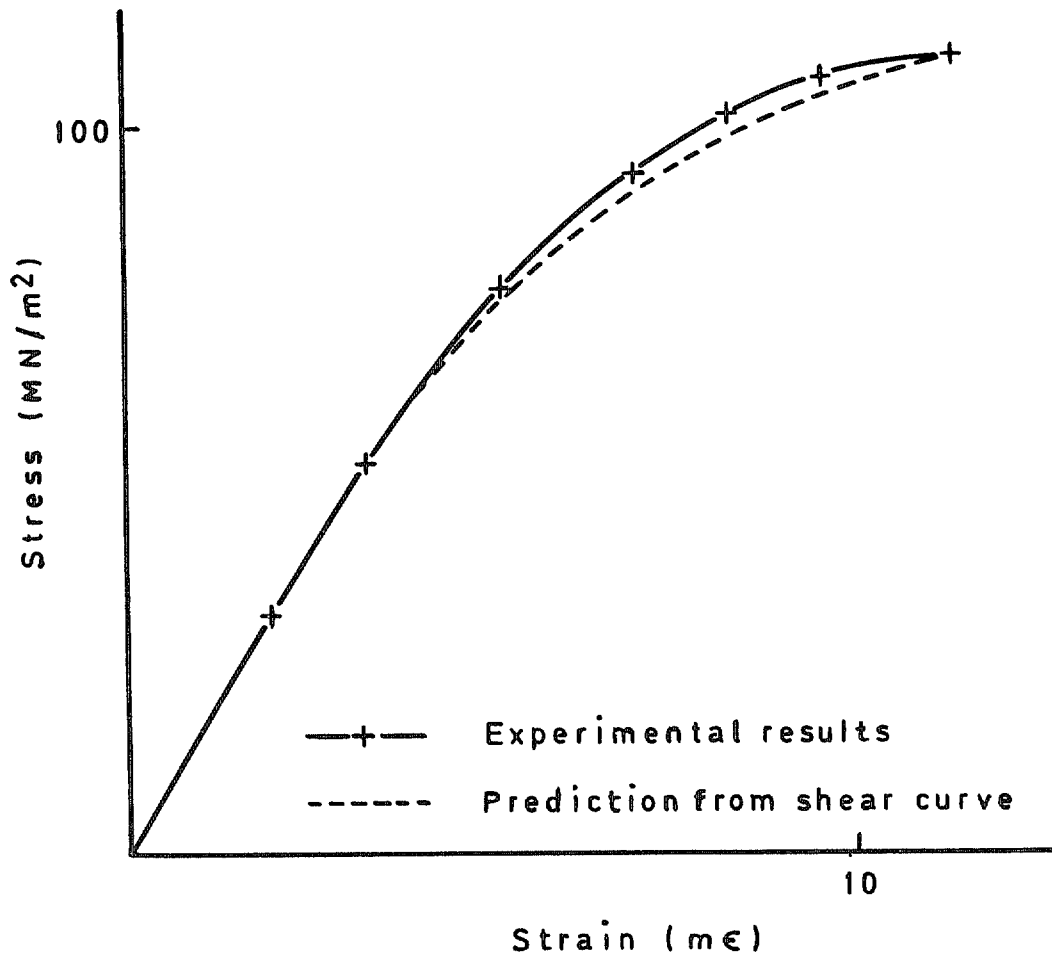


Fig 12 Tensile response of a  $\pm 45^\circ$  high strength (HT-S) angle-ply laminate: experimental results and prediction from unidirectional shear stress/strain curve

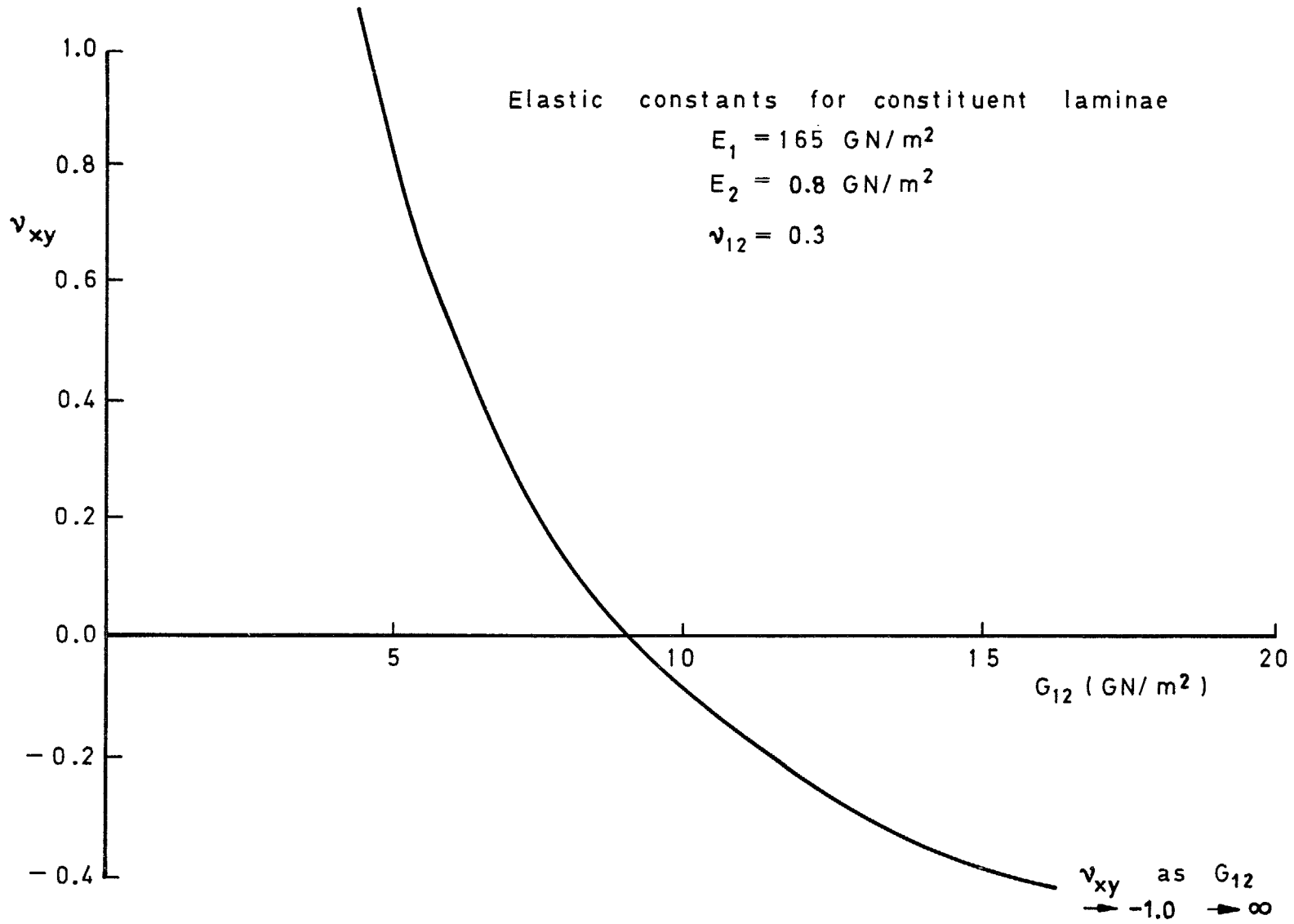


Fig 13 Variation of  $\nu_{xy}$  with  $G_{12}$  for a  $\pm 45^\circ$  high strength (HT-S) angle-ply laminate (Equation (31))

R & M No. 3816

© *Crown copyright*

1978

Published by  
HER MAJESTY'S STATIONERY OFFICE

*Government Bookshops*  
49 High Holborn, London WC1V 6HB  
13a Castle Street, Edinburgh EH2 3AR  
41 The Hayes, Cardiff CF1 1JW  
Brazenose Street, Manchester M60 8AS  
Southey House, Wine Street, Bristol BS1 2BQ  
258 Broad Street, Birmingham B1 2HE  
80 Chichester Street, Belfast BT1 4JY  
*Government Publications are also available  
through booksellers*

HMSO

R & M No. 3816  
ISBN 0 11 471149 6